UC Berkeley
UC Berkeley Electronic Theses and Dissertations

Title
Mechanisms of Heterochromatin Silencing in *Saccharomyces cerevisiae*

Permalink
https://escholarship.org/uc/item/87q1494q

Author
Steakley, David Lee

Publication Date
2013

Peer reviewed|Thesis/dissertation

eScholarship.org Powered by the California Digital Library
University of California

Mechanisms of Heterochromatin Silencing in *Saccharomyces cerevisiae*

By

David Lee Steakley

A dissertation submitted in partial satisfaction of the

requirements for the degree of

Doctor of Philosophy

in

Molecular and Cell Biology

in the

Graduate Division

of the

University of California, Berkeley

Committee in charge:

Professor Jasper Rine, Chair
Professor Michael Levine
Professor Barbara Meyer
Professor Robert Fischer

Fall 2013

Mechanisms of Heterochromatin Silencing in *Saccharomyces cerevisiae*

© 2013

David Lee Steakley

Abstract

Mechanisms of Heterochromatin Silencing in *Saccharomyces cerevisiae*

by

David Lee Steakley

Doctor of Philosophy in Molecular and Cell Biology

University of California, Berkeley

Professor Jasper Rine, Chair

Sir proteins are responsible for maintaining stable transcriptional repression and silencing of telomeres, rDNA, and silent mating-type loci in *S. cerevisiae*. Decades of research identify a thorough list of the proteins required to establish and maintain silencing at *HML* and *HMR,* but despite many models being put forward, the mechanism by which Sir-proteins repress transcription has not been definitively determined. I sought to determine the mechanism of transcriptional silencing within heterochromatin in yeast.

I tested models of transcriptional silencing using a variety of orthogonal *in vivo* approaches to build a more comprehensive model of the mechanism of silencing by Sir proteins. Specifically, I assayed for RNA Pol II in an engaged, DNA-melted form at the promoter of *HML**α***1 to conclusively test predictions of the downstream-inhibition model. I then adapted the single-subunit RNA polymerase of T7 phage and its cognate promoter to test the ability of a silenced template to be transcribed by a heterologous transcription assay *in vivo*. Finally, I adapted the thoroughly studied *GAL1* promoter and Gal4 activator to test whether the extent of repression by Sir-proteins at *HMR* is sensitive to the nature of the transcription factor or to the promoter being repressed.

These studies provided a framework for understanding the mechanism of Sir-protein repression. I propose a dynamic affinity-based competition model for transcriptional silencing where Sir proteins primarily restrict transcription before RNA Polymerase II has melted DNA at its target and competition between Sir proteins and gene-specific activators at promoters determines the efficiency of silencing.

Contents

Contents i

Acknowledgements iii

Chapter 1: Introduction to transcriptional repression, silencing and chromatin in *Saccharomyces cerevisiae* 1
- *Figure 1.1*: *Mating-type loci of chromosome III* 3

Chapter 2: Mechanisms of Sir-based heterochromatin silencing in *Saccharomyces cerevisiae* 10
- Introduction 10
- Results 11
  - *Figure 2.1*: The $KMnO_4$ reactivity of *HMLα1 in vivo* 13
  - *Figure 2.2*: Assays of transcription and translation for *HMR T7pro::a1* 16
  - *Figure 2.3*: Transcript analysis of *HMR T7pro::a1* upon kinetic induction of T7 RNA polymerase in *SIR4* and *sir4*Δ strains 18
  - *Figure 2.4*: 13xMYC-Sir3 enrichment at *HMR* and telomere V R upon kinetic induction of T7 RNA polymerase in *SIR4* strains 19
  - *Figure 2.5*: 13XMYC-Sir3 enrichment at *HMR T7pro::a1* lacking T7 RNA polymerase as assayed by ChIP followed by high-throughput sequencing 21
  - *Figure 2.6*: Assays of transcription and translation for *HMR GAL1pro::a1* 23
  - *Figure 2.7*: mRNA analysis of *HMR GAL1pro::a1* upon kinetic induction of T7 polymerase in *SIR4* and *sir4*Δ strains 24
  - *Figure 2.8*: 13xMYC-Sir3 and Gal4 enrichment at *HMR GAL1pro::a1* upon kinetic galactose induction in *SIR4* strains 25
  - *Figure 2.9*: Gal4 enrichment at *HMR GAL1pro::a1* and *GAL1* upon kinetic galactose induction in *SIR4* and *sir4*Δ strains 27
  - *Figure 2.10*: mRNA analysis of Gal4 wild-type and gal4L331P and effects on transcriptional activation and silencing at *HMR GAL1pro::a1* 27
- Discussion 28
- Materials and Methods 32
  - *Table 2.1*: Yeast strains 36
  - *Table 2.2*: Yeast and bacterial plasmids 37
  - *Table 2.1*: Oligonucleotides 37

References 40

Appendix I: A novel genetic interaction between *SIR2* and the *ASF1, RTT109* histone acetylation and incorporation pathway 50
- Introduction 50
- Results 51
  - *Table AI.1*: Results of *sir2*Δ-synthetic-genetic-interaction-tetrad analysis 52
  - *Figure AI.1*: *sir2*Δ-synthetic-genetic-interaction-tetrad analysis images 53
  - *Figure AI.2*: Growth rates of *sir2*Δ, *rtt109*Δ, and *asf1*Δ mutants in rich media liquid culture 54

Table AI.2: ε-values calculated based on kinetic growth rate 55
Table AI.3: *sir2*Δ-synthetic-genetic interactions assayed by tetrad analysis 55
Figure AI.3: Growth rates of *sir2*Δ, *rtt109*Δ and *asf1*Δ mutants in rich and 5mM nicotinamide media liquid culture 57
Discussion 57
Materials and Methods 59
TableAI.4: Appendix yeast strains 60
TableAI.5: Appendix oligonucleotides 63
Appendix references 64

Acknowledgements:

I first thank my advisor, Jasper Rine, for his limitless encouragement, guidance, patience, and support during my time in his lab. I could not have found a better graduate mentor. Jasper continuously demonstrated his deep investment in the professional and personal growth of his trainees. I thank him for my development as an analytical thinker and an experimentalist. Jasper is an example to follow in all areas of scholarship from the actual practice of genetics, to service and teaching. I will count my future career as a success if I can emulate even a small number of Jasper's great qualities as a scientist and mentor. So, to Jasper a heartfelt thank you for everything you have done and continue to do for me.

I thank my thesis committee, Barbara Meyer, Mike Levine, and Bob Fischer. Throughout my graduate career they provided insightful comments and suggestions that greatly improved the quality of my science and my thinking.

I cannot imagine my time in graduate school without the friendship and support of my labmates. Together they filled my time in the Rine lab with humor and camaraderie. It was a pleasure to come to work everyday with such a brilliant and fun group of people. I was drawn to the Rine lab for its overwhelmingly positive culture. Its great atmosphere will be one of my fondest memories. I thank the following Rine Lab members for their friendship and for always having the time to share their expertise with me. Lenny, Bilge, Jake, Jen, Erin, Oliver, Laura, Rachel, Jeff, Nick, Dago, Kripa, Meara, Jean, Jessica, Lauren, Sarah, Katie H., Katie S., David, Aisha, and Anne thank you all. You were all the best crash of "Rine-os" I could imagine.

I give a special thanks to my two best friends in lab Meru Sadhu and Debbie Thurtle. Because they joined the lab directly before and after me, I spent almost my entire graduate career with them. They are life-long friends. I conservatively estimate I have spent around 5% of my life with them in 392 Stanley Hall. I could always count on them to commiserate about and then troubleshoot a failed experiment or celebrate a successful one. We supported each other in the process of navigating graduate school, and for that they will always hold a special place in my thoughts. To the three musketeers and Daru!

The work discussed in the appendix was undertaken with a talented undergraduate, Justin Feng. He was the first undergraduate student I worked with, and he set the bar high. He is a smart, diligent, and self-motivated experimentalist. I look forward to hearing about all of his future successes.

I also want to recognize my family of teachers for creating an environment that valued learning and education. I would not be where I am today if we didn't "always have money for books". Thank you for always maintaining high expectations and pushing me to go beyond average.

Special thanks to David Barrington at the University of Vermont for providing me my first research experience and helping me to become a real “knees in the dirt” biologist and naturalist. He showed me how to connect biological knowledge to organisms living in the woods and nature. I would not have considered a career in research science without his encouragement.

I thank my high school science teachers, Ms. Krashes, Mr. Witherow, Ms. Gingras, Mr. Thorp and most importantly Mr. Buell. They were the first people to introduce me to the beauty of science as a way of investigating the world. Their work often goes unappreciated, but their teaching and guidance had a profound effect on the direction of my life and I want to formally recognize and thank them for that.

I also acknowledge the important roles that the taxpayer and the government play in funding and promoting science research in the United States. This thesis is based upon work supported by the National Science Foundation Graduate Research Fellowship under grant number (DGE 1106400) as well as the NIH Institute of General Medical Science under grant number (RO1 GM031105-28).

Lastly I want to thank my wife and best friend Maggie for her ceaseless encouragement, quiet patience, and unwavering love. She supported me through every step of graduate school and put up with me as I navigated rotations, prepared for and took my qualifying exam, performed 36-hour experiments, worked on holidays, and prepared my thesis. Her support, belief, and confidence in me make everything else I do possible.

Chapter 1: Introduction to transcriptional repression, silencing and chromatin in *Saccharomyces cerevisiae*

The human body contains at least 140 classically-recognized cell types, and more continue to be discovered. With a small number of exceptions, such as T cells and B cells, it is generally assumed that all cells in any individual have the same DNA sequence within its nucleus. How do cells in one organism establish and maintain such vastly different identities in both form and function when they have the same DNA sequence? The incredible complexity of multicellular organisms inspires such a question, but we can investigate the fundamental principles underlying the establishment of different cell fates with fewer confounding complications in the single-celled eukaryote, budding yeast, *Saccharomyces cerevisiae*.

Wild-type haploid yeast cells exist as either a or **α** mating-types, though each cell contains the genetic information necessary to adopt both cell types. Gene regulation mechanisms allow cells to make decisions about what genes to express or repress at different positions in the genome or in response to specific developmental or environmental cues, to arrive at specific cellular phenotypes.

In yeast, the process of transcriptional silencing represses some copies of the genes required to specify mating-type identity. Transcriptional silencing is a form of regional, promoter-independent repression, mediated by the Silent Information Regulator (SIR) protein complex. Transcriptional silencing results in a 1000-fold reduction in transcript levels of mating-type genes at two positions in the genome, *HML* and *HMR*, compared to expression of those same genes at a different locus, *MAT*. For this thesis, I have focused on understanding the molecular mechanism by which transcriptional silencing dramatically blocks transcription. Broadly, I hope to explain how an evolutionarily conserved repression mechanism restricts transcription of a gene as a function of its position in the genome. As an introduction to this dissertation, this chapter contains a brief description of transcription in yeast followed by a review of transcriptional silencing in yeast, including the associated chromatin biology. This introduction will set the stage for an understanding of the various ways in which transcriptional silencing may block transcription as a prelude to the mechanistic studies presented in Chapter 2.

Gene Regulation in Yeast

The yeast *Saccharomyces cerevisiae* is a well-established, genetically-tractable, and popular organism for the study of gene regulation. Numerous studies that identified and characterized conserved gene regulatory programs were first carried out in yeast. Examples include daughter-cell-specific repression (reviewed in (Cosma, 2004)), or the modulation of chromatin structure in response to environmental conditions such as phosphate regulation (reviewed in (Musladin and Barbarić, 2010)). Much of the fundamental work on eukaryotic

transcriptional activation is based on the studies of yeast RNA polymerase II both *in vivo* and *in vitro* (Flanagan et al., 1990; Lorch et al., 1992; Kornberg, 2007). Yeast also employs classic examples of promoter-specific repression such as repression mediated by DNA binding proteins that then recruit the Tup1/Ssn6 complex and associated histone deacetylases as co-repressors (Parnell and Stillman, 2011). The finding that mating-type identity in yeast is mediated by a promoter-independent, transcriptional silencing also established yeast as a model for the study of regional repression (Haber and George, 1979; Klar et al., 1979; Rine et al., 1979; Rine and Herskowitz, 1987).

Transcriptional silencing and Sir proteins help maintain cell identity

The mating type of wild-type haploid yeast can be either a or **α** depending on the allele, *MATa* or MAT**α**, at the expressed *MAT* locus on chromosome III. A copy of both a-mating type and **α**-mating type information is contained at *HMRa* and *HML**α***, respectively, near the ends of chromosome III. *HMRa* and *HML**α*** are both normally silenced (Figure 1.1), (Herskowitz, 1988). A screen performed to identify factors required to maintain the silent state of *HM* loci identified four *SIR* genes that were required or important (Rine and Herskowitz, 1987). The four Sir proteins are present throughout the silent loci as detected by chromatin immunoprecipitation (ChIP) studies (Rusche et al., 2002). ChIP followed by high-throughput sequencing data (ChIP-Seq) appears to show a heterogeneous distribution of Sir proteins throughout *HML* and *HMR*. However, careful analysis of the impact of cross-linkers on nucleosome detection in silenced chromatin reveals that Sir proteins are likely distributed evenly, but crosslinking keeps the ChIP-Seq method from recovering specific sequences in silenced chromatin (Thurtle and Rine, 2013 submitted). The association of Sir proteins is easily detected at the silencers, named *E* and *I*, flanking *HML* and *HMR*, because the Sir proteins associate with the three proteins that bind silencer elements: the two sequence-specific transcription factors, Abf1 and Rap1, and the Origin Recognition Complex, ORC, which recruit Sir proteins, thus initiating the assembly of silent chromatin. In cells lacking *SIR2*, *SIR3* or *SIR4, HML and HMR* loci are depressed. Haploid yeast with such mutations adopt a pseudo-diploid phenotype of an a/**α** diploid, and lose the ability to mate. Deletion of *SIR1* eliminates functional silencing at *HML* in only 80% of cells within a population. The other 20% of cells maintain silencing and most often give rise to silenced daughter cells. This phenotype results in clonal populations of genetically identical cells in a *sir1*Δ culture that exist in either the silenced or derepressed state. Transitions between these two states occur at low frequencies (Pillus and Rine, 1989; Xu et al., 2006). These transitions from the derepressed to the silenced state have made *sir1*Δ mutants useful in examining *de novo* silencing establishment.

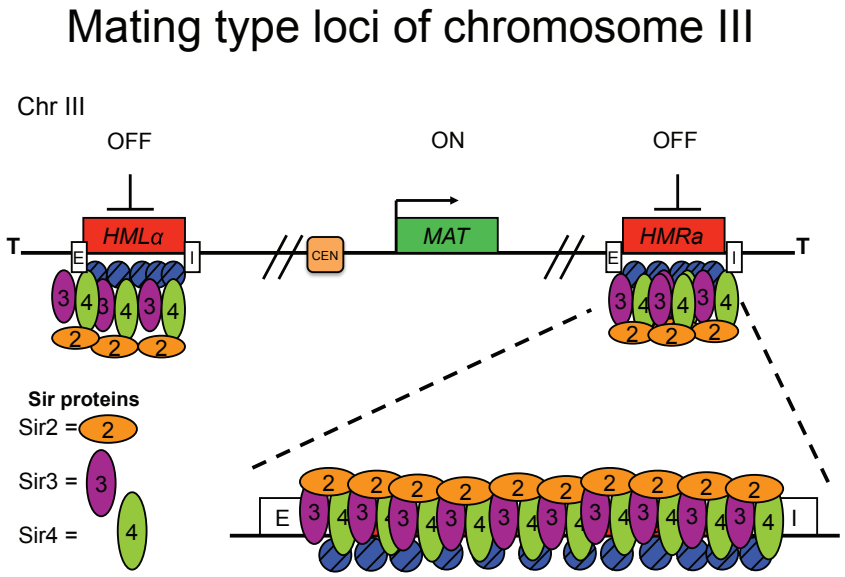


Figure 1.1: Mating-type loci of Chromosome III
The expressed allele of mating type information resides at *MAT* while *HML**α*** and *HMRa* are silenced by Sir proteins. Silencers elements (E and I) are shown flanking repressed *HML**α*** and *HMRa* and contain binding sites for ORC (ACS), Abf1, or Rap1. Nucleosomes bound and deactylated by Sir proteins are shown throughout the silenced loci.

Sir proteins repress recombination and are present at telomeres and rDNA

Sir proteins are also present at telomeres through interactions with numerous Rap1 proteins whose binding site is present in many copies in the repeated sequence made by yeast telomerase. Sir4 interacts with Rap1 and mediates the recruitment of the entire Sir2/3/4 complex to telomeres (Hecht et al., 1996; Moretti et al., 1994). Sir4 also associates with the DNA end-binding protein Ku (Mishra and Shore, 1999), which is present at telomeres. The recruitment of the Sir 2/3/4 complex to telomeres can result in the silencing of reporter genes placed in close proximity (Gottschling, 1992; Gottschling et al., 1990). Evidence from ChIP and ChIP-seq analyses demonstrates that the silenced domain does not extend further than 2kb in wild-type cells, except on chromosome III, where it appears to extend from *HML* to the left telomere (Zill et al., 2010). Overexpression of Sir3 can extend the sub-telomeric-silencing domain, and silence reporter genes placed further away from telomeres (Hecht et al., 1996). The Sir 2/3/4 complex silences transcription at telomeres at least in part by preventing the binding of RNA polymerase II (Kitada et al., 2012), but its action at telomeres may also be important beyond silencing as a reservoir of additional Sir-complexes for silencing at *HML* and *HMR* loci (reviewed in (Talbert and Henikoff, 2006)).

Other yeast such as *Candida glabrata*, a human pathogen, use Sir proteins for the condition-specific repression of a family of subtelomeric *EPA* genes which mediate adhesion. When *C. glabrata* cells are present in urine prior to being evacuated, they experience decreased nicotinic acid concentrations, relative to levels of nicotinic acid in the blood. Decreased nicotinic acid and the resulting decreased intracellular NAD+ concentrations limit catalysis of Sir2 because Sir2 consumes NAD as part of its enzymatic mechanism. Thus, silencing is compromised and the *EPA* genes are expressed. *EPA* gene expression dramatically increases the stickiness of the cells and helps prevent the pathogen from being evacuated (Domergue et al., 2005). In contrast, a pathogen in the blood stream is better able to disseminate when its adhesion proteins are silenced, made possible by the elevated NAD levels in *Candida* cells in the blood stream. In this case condition-dependent transcriptional silencing is used as a gene regulatory mechanism to prevent or allow expression of protein coding genes at telomeres depending on environmental conditions.

Sir2 is also present at the rDNA in *S. cerevisiae*. The rDNA locus in yeast consists of approximately 150-200 rDNA repeats on chromosome XII. This locus is bound by the RENT complex, consisting of Sir2, Cdc14 and Net1 (Straight et al., 1999). This complex binds to the rDNA to prevent intra-chromatid recombination between repeats (Huang and Moazed, 2003). Strains deleted for *SIR2* display an expansion of rDNA repeat numbers and an increase in the number of Extra-chromsomal rDNA Circles (ERCs) (Park et al., 1999). In *S. cerevisiae,* the accumulation of ERCs accelerates replicative aging and has a fitness cost (Sinclair and Guarente, 1997). Pol II transcribed genes placed within

the rDNA locus are silenced in a Sir2-dependent manner, but Pol I transcription itself is not (Smith et al., 1998). Thus, the primary role of Sir2 at the rDNA is in repressing recombination and maintaining genome integrity.

The Sir-complex is also important for regulating recombination during mating-type switching. Mating-type switching begins when the *HO* endonuclease, expressed specifically in experienced mother cells, makes a Double-Strand Break (DSB) at its recognition site in *MAT*. This DSB then precipitates DNA resection and a homology search to locate a homologous DNA sequence, eventually finding such sequences present at *HML* or *HMR*. The allele at *HML* or *HMR* then acts as the repair template, and usually the opposite mating-type allele is copied into the expressed *MAT* locus. This switches the expressed mating type in the mother cell allowing it to mate with nearby haploid cells, like its recently divided daughter. A finely-controlled mechanism ensures that cells choose the donor locus of the opposite mating type to repair the DSB at *MAT* (Li et al., 2012). Importantly, HO only cuts at the active *MAT* locus, and not at the silenced *HML* and *HMR* loci because the Sir proteins block access of the HO endonuclease to its recognition sequence at *HML* and *HMR.* Thus, the Sir proteins at *HML* and *HMR* ensure the cell does not have to repair multiple DSBs, a process that could lead to incorrect or unresolvable recombination products, and gives directionality to the mating-type switching by maintain the distinction between donor and recipient loci (reviewed in (Haber, 1998)).

Binding of Sir proteins changes the properties of silenced loci

There are dramatic molecular differences between euchromatin at *MAT* and heterochromatin at *HML* and *HMR* in wild-type cells. These differences result from the binding and action of the Sir proteins, because in *sir* mutants the chromatin at *HML* and *HMR* is indistinguishable from that at *MAT*. Euchromatin is characterized by its openness and accessibility to a variety of DNA binding factors, transcription factors and RNA polymerase (Chen and Widom, 2005), and the presence of activating histone modifications associated with transcription, such as specific sites of histone acetylation and methylation on H3 and H4 tails. Heterochromatin is characterized as being closed or condensed, less accessible to DNA binding proteins, transcription factors (Loo and Rine, 1994), and RNA polymerase machinery (Chen and Widom, 2005). Heterochromatin at *HML* and *HMR* also has highly positioned nucleosomes (Weiss and Simpson, 1998; Ravindra et al., 1999) and is depleted for activating histone modifications (Waterborg, 2000; Bernstein et al., 2002). Sir2, the catalytic component of the Sir-complex responsible for creating heterochromatin in yeast, is a NAD-dependent histone deactylase and specifically deactylates H4K16-Ac as well as H3K9-Ac and H3K14-Ac (Park and Szostak, 1990; Imai et al., 2000; Landry et al. 2000).

The exact proteins required by the Sir-complex to repress target loci are specific to *S. cerevisiae*, even among its close relatives (Zill et al., 2010).

However, the use of chromatin binding/modifying proteins to modulate transcription is pervasive in eukaryotes. Recent studies demonstrating examples of this method of regulation include Polycomb repression in flies (Dellino et al., 2004), PHD-containing proteins in Arabidopsis binding H3K4me3 (la Paz Sanchez and Gutierrez, 2009), Set-domain proteins and H3K4me3 in *S. cerevisiae* (Nislow et al., 1997), and *SWI6*/HP1 in *S. pombe* (Canzio et al., 2011).

Cytologically, heterochromatin appears condensed and is associated with the nuclear periphery. It is unclear whether this localization causes any of the properties of heterochromatin or is a consequence of these properties. Tethering a euchromatin domain to the nuclear periphery does not necessarily cause silencing, nor does disruption of periphery localization necessarily disrupt silencing (Gartenberg et al., 2004; Gasser et al., 2004). Chromosome-conformation-capture assays detect associations between silencer elements of *HML* and *HMR* in both *cis*, between the two silencers at either *HML* or *HMR,* and *trans*, between *HML* and *HMR* silencers together (Valenzuela et al., 2008; Miele et al., 2009). Additionally, the highest peaks of Sir protein ChIP-Seq enrichment occur at silencers, consistent with their tight association with Sir proteins (Thurtle and Rine, 2013 under review).

Assembly of the Sir-complex on silenced loci

To silence transcription, Sir proteins must assemble into a functional Sir-complex and then create a repressive chromatin structure on a target locus. This process begins with the binding of sequence-specific transcriptional activators Abf1, Rap1, and the Origin Recognition Complex at their binding sites present at silencers. The *HMR* E silencer contains binding sites for Rap1, Abf1, and ORC. Both I silencers at *HML* and *HMR* are bound by Abf1 and ORC, whereas *HML* E is bound by Rap1 and ORC. Once these sequence-specific proteins are bound to silencers, they first recruit Sir1 and then other members of the Sir-complex (Moretti et al., 1994; Triolo and Sternglanz, 1996; Fox et al., 1997; Moazed et al., 1997; Hoppe et al., 2002; Rusche et al., 2002). The presence of the silencers is a key factor in silencing because they position the initial binding of the Sir-complex, which then deacetylates nucleosomes within *HMR* and *HML*. The conserved position of the silencers at *HMR* and *HML* within the *Saccharomyces sensu stricto* clade supports this idea (Teytelman et al., 2008).

Both Sir protein binding and the catalytic activity of Sir2 are required to silence transcription. Mutants in the catalytic domain of Sir2 disrupt silencing and have a phenotype indistinguishable from that of a null mutant (Imai et al., 2000). Sir3 and Sir4 make important contacts with each other to assemble a stable Sir2/3/4-complex, as well as with nucleosomes to anchor the Sir2/3/4-complex on chromatin (Armache et al., 2011). The binding interactions between Sir3, Sir4, and nucleosomes are also required for silencing, as mutations that disrupt these contacts lead to silencing defects (Kayne et al.,1988; Park et al., 2002; Ehrentraut et al., 2011). The current model of silencing establishment features

sequential, stepwise spreading of Sir protein complexes based on their higher affinity for deactylated H3/H4 tails, created by the catalytic activity of Sir2, than for acetylated H3/H4 tails (Rusche et al., 2002). It remains unclear if the mechanism by which Sir proteins assemble to coat a locus is necessarily stepwise on adjacent nucleosomes or whether a Sir-protein complex can deacetylate and bind nearby nucleosomes without requiring them to be immediately adjacent.

The time required to silence a locus varies depending on the assay. In batch culture with an inducible allele of Sir3, Sir3 silences transcription of *a1* mRNA after 60 minutes (Lynch and Rusche, 2008). When monitoring individual cells by their ability to respond to mating pheromone, addition of Sir3 to a *sir3*Δ cell leads to repression after on average two cell divisions, or roughly 180 minutes (Osborne et al., 2009).

The effect of chromatin structure on silencing

The position of nucleosomes also plays a large role in gene regulation. Nucleosomes have been coined as the "original repressor". In some cases targeting a chromatin remodeler to a locus, thus altering nucleosome positioning, is enough to allow transcription (Whitehouse et al., 2007). If nucleosomes stably occupy specific positions necessary for RNA polymerase and the transcription-associated factors (TAFs), then a Pre-initiation complex (PIC) cannot be formed until the nucleosomes are repositioned. If the PIC is present, the positioning of surrounding nucleosomes may reduce the ability of elongation factors to bind. The position of nucleosomes at *HML* and *HMR* as determined by DNAse footprinting show that the transcription start sites of the *a1* and *a2* genes, within *HMR,* are covered by stably-positioned nucleosomes (Ravindra et al., 1999; Weiss and Simpson, 1998). These data suggest that nucleosomes may play a direct role in excluding transcription machinery or restricting transcription. *HMR* provides an excellent locus to test this hypothesis because of its smaller size and regular nucleosome distribution.

The mechanism of silencing

The transcription cycle can be regulated at any of the steps within the cycle: DNA or chromatin state (Mai et al., 2000), promoter accessibility (Fascher et al., 1993), transcription factor or repressor binding (Um et al., 1995), preinitiation-complex formation (Olave et al., 1998), initiation (Hengartner et al., 1998), the transition to productive elongation (Zeitlinger et al., 2007), and termination (Padmanabhan et al., 2012). Furthermore, even after the nascent or complete RNA is transcribed it can be degraded by the exosome (van Dijk et al., 2012). Repressive mechanisms could operate at any of these individual steps.

The silencing field has a good understanding of the DNA and protein elements required to silence transcription, and of the phenotypic consequences

of disrupting silencing. However, the mechanism by which Sir proteins and heterochromatin block transcription remains contentious. *In vitro* studies show that deactylation of histones condenses chromatin fibers (Shogren-Knaak et al., 2006). Thus, Sir proteins, by deacetylating histones H3 and most importantly, H4K16, at silent loci could sterically occlude sequence-specific binding proteins, effector proteins, or transcription machinery by a condensation mechanism. Indeed, silenced chromatin within *HMR* is refractory to sequence-specific restriction enzymes relative to the same locus in Sir- cells (Loo and Rine, 1994). Likewise, telomeric chromatin is more resistant to modification by DNA methyltransferases than euchromatin (Gottschling, 1992). The Widom lab challenged this model, reporting that the block to transcription at *HMR* occurs by occluding the preinitiation-complex more thoroughly than it occludes other sequence-specific binding proteins and may depend on nucleosome position (Chen and Widom, 2005). Importantly, they demonstrate that a variety of non-transcription proteins directed to sequences within *HML* and *HMR* (Lex-A, DAM methylase) show only a small reduction in accessibility within silenced chromatin relative to the same sequences in active chromatin. The magnitude of these effects in their study would not adequately explain the dramatic reduction in transcript levels observed by RNA analysis. Their work also finds that RNA polymerase II (RNA Pol II) is absent from silenced loci by ChIP analysis. Work from the Grunstein group supports this conclusion, suggesting that teleomeric gene silencing in yeast largely prevents RNA Polymerase II binding (Kitada et al., 2012). In contrast, the Gross lab has reported that RNA Polymerase II is present at various silenced loci by ChIP analysis, yet these loci do not produce functional mRNAs (Gao and Gross, 2008). They conclude that promoters within silenced loci remain accessible to RNA Polymerase II (Sekinger and Gross, 2001), and that inhibition of transcription occurs in Sir-based heterochromatin downstream of preinitiation-complex assembly. The literature refers to this idea as “the downstream-inhibition model”. However, D. Gross does not currently support the downstream inhibition model (personal communication). Recent publications by the Moazed lab suggest, based on *in vitro* reconstitution of recombinant Sir-protein coated chromatinized linear DNA fragments, that a Gal4-VP16 activator is able to bind within silenced domains, but coactivator-complex binding is inhibited by Sir proteins. Additionally, they report that heterochromatin also acts as a barrier to elongation (Johnson et al., 2009; 2013). This model incorporates elements of the “PIC interference” and the “downstream inhibition” model to account for the quantitative efficiency of silencing.

The experiments presented in this thesis, in conjunction with published literature mentioned above and a variety of whole-genome analyses, (Steinmetz et al., 2006; Nagalakshmi et al., 2008) highlight the debate surrounding the mechanism by which Sir-silenced chromatin restricts transcription. Does heterochromatin: (1) sterically prevent assembly of transcription factors at promoters, (2) keep RNA polymerase from reaching productive elongation, (3) prohibit further extension of mRNA transcripts, (4) act by another mechanism all together, or (5) result from a combination of these influences? Resolving these

inconsistencies has implications beyond basic research, due to the importance of heterochromatin in many processes, including X-inactivation in mammals (Heard et al., 2001), misregulation of heterochromain domains in cancers (Pruitt et al., 2006), and immune evasion mediated by Sir proteins in unicellular pathogens such as Plasmodium and Trypanosomes (Deitsch et al., 1999).

This dissertation addresses a fundamental question about gene regulation and transcription: what is the molecular mechanism by which Sir proteins and heterochromatin block transcription? It is my intention to more completely describe an important gene regulation paradigm to resolve its mechanistic basis.

Chapter 2: Mechanisms of Sir-based heterochromatin silencing in *Saccharomyces cerevisiae*

Introduction:

All eukaryotic organisms transcribe DNA from a chromatin template, and thus the state of the local chromatin environment plays a role in modulating gene expression. Highly condensed chromatin that is transcriptionally inactive is called heterochromatin. Transcriptional silencing is a form of heterochromatin-based, regional, promoter-independent repression, mediated in *Saccharomyces cerevisiae* by the Silent Information Regulator (SIR) protein complex. Sir-protein based transcriptional silencing represses auxiliary copies of the genes that specify mating-type identity. Transcriptional silencing results in a 1000-fold reduction in transcript levels of mating-type genes at two positions in the genome, *HML* and *HMR*, compared to expression of those same genes at the active *MAT* locus.

The DNA elements and proteins required to establish and maintain silencing have been identified (reviewed in (Rusche et al., 2003)). Silencing of transcription requires the recruitment of the Sir2/3/4-complex to silencers, the catalytic activity of Sir2, a histone deacetylase (Imai et al., 2000; Landry et al., 2000), and the spreading of the Sir2/3/4-complex across a locus to establish a repressive chromatin domain (Rusche et al., 2002). The molecular mechanisms by which the binding of the Sir proteins and the establishment of a silenced local chromatin domain repress transcription are the subject of this chapter.

Three models for how Sir proteins silence transcription have been put forth over the past 20 years. The steric occlusion model is based upon silenced chromatin's ability to block binding of sequence-specific DNA binding proteins to their binding sites in silenced chromatin (Strathern et al., 1982; Gottschling, 1992; Loo and Rine, 1994). Thus, Sir proteins create a specialized local chromatin structure that is broadly inaccessible to site-specific DNA-binding proteins and, by extension, the transcription machinery.

The preinitiation-complex interference model is a refinement of the steric occlusion model. The preinitiation-complex interference model is based on quantitative analysis of the effect of Sir proteins on restricting access of site-specific DNA binding proteins and ChIP data showing the absence of general transcription machinery, TFIIB (Sua7), TFIIE (Tfa2), and, RNA Pol II (Rpb1) from heterochromatin. In contrast, Ppr1, the gene-specific activator for a silenced *URA3* transgene, is present within heterochromatin and only slightly reduced in occupancy, dependent on the presence of Sir proteins (Chen and Widom, 2005). The preinitiation-complex interference model suggests that the quantitative reduction in access of DNA binding proteins within heterochromatin is too small to account for the 1000-fold reduction in transcription due to silencing. Therefore, the phenotypic reduction in transcription due to silencing results from

specific factors within the preinitation-complex being blocked from accessing their target sites, preventing the formation of a preinitation-complex and thus blocking transcription. Importantly, the data that led to this model show by ChIP that RNA Pol II, as well as TFIIB and TFIIE, are absent from silenced heterochromatin at *HML* and *HMR*. Another more recent study also concludes that RNA Pol II is absent at silenced telomeres (Kitada et al., 2012).

In contrast to the previous two models, the downstream-inhibition model is supported by claims that RNA Pol II is present in silenced chromatin and can melt DNA, but is blocked by Sir proteins before it can elongate and complete productive transcription. The downstream-inhibition model is based on ChIP data interpreted as showing that RNA Pol II and components of the preinitation-complex, TBP (Spt15) and TFIIH (Tfb1, Kin28), are localized to silenced and active chromatin roughly equally, but mRNA capping proteins (Cet1, Abd1) and downstream elongation factors (Spt5, TFIIS, Paf1) are specifically absent (Gao and Gross, 2008). In support of this observation, gene-specific activators and RNA Pol II are reported to be localized to *HSP82* placed adjacent to, and silenced by, *HMR-E* (Sekinger and Gross, 2001). Whole-genome studies also suggest that RNA Pol II may be present in heterochromatin (Steinmetz et al., 2006).

These models, and the data supporting them, present clear contradictions. I tested these models of silencing using a variety of orthogonal *in vivo* approaches to build a more comprehensive model of the mechanism of silencing by Sir proteins. Specifically, I assayed for RNA Pol II in an engaged, DNA-melted form at the promoter of *HML* to conclusively test predictions of the downstream-inhibition model. I then adapted the single-subunit RNA polymerase of T7 phage and its cognate promoter to test the ability of a silenced template to be transcribed by a heterologous transcription assay *in vivo*. Finally, I adapted the thoroughly studied *GAL1* promoter and Gal4 activator to test whether the extent of repression by Sir proteins at *HMR* is sensitive to the nature of the transcription factor or to the promoter being repressed.

Results:

Stalled polymerase is not present at *HMLα1*

The process of transcription involves an orderly cascade of protein-binding events, initially at promoters and later, in the bodies of genes. To achieve productive transcription a complete preinitiation-complex, including RNA Pol II bound on a core promoter, is assembled. Then transcription can be initiated by phosphorylation of RNA Pol II on Ser5 of the carboxyl terminal domain of Rpb1 by TFIIH (Kin28). Completion of these steps allows the polymerase to melt its DNA template and begin to transcribe, moving into early elongation. In early elongation, RNA polymerase II opens the DNA duplex and begins to transcribe between 5-50 nucleotides before the transcription stalls at an mRNA capping

checkpoint. Upon the binding of specific checkpoint and elongation factors, RNA polymerase proceeds to productive elongation (reviewed in (Lee and Young, 2000)). The sequential nature of the transcription cascade establishes a temporal order, and a block at one step of the process necessarily prevents subsequent events from occurring.

The ChIP data that supports the downstream-inhibition model show that all preinitiation-complex factors tested, including TFIIH (Kin28) and RNA Pol II, are enriched at roughly equal levels in active or silent chromatin. The first general transcription factors in the transcription cascade missing from silent chromatin, but present in euchromatin, are Cet1 and Abd1, members of the mRNA capping checkpoint (Gao and Gross, 2008). The downstream-inhibition model implies that RNA polymerase is present in silenced chromatin on the template, stalled on melted DNA strands, and awaiting the action of Cet1 and Abd1 to move into productive elongation.

I tested this prediction using an *in vivo* potassium permanganate assay at *HML**α**1*. Potassium permanganate preferentially reacts with and modifies T residues in single-stranded DNA (Rubin and Schmid, 1980) and can be used to detect stalled RNA polymerases that have melted the DNA template and opened a characteristic transcription bubble, but have not proceeded into productive elongation (Giardina et al., 1992). The background reactivity of naked DNA *in vitro* was highly similar to the reactivity *in vivo* from *SIR4* samples. I saw no characteristic stalled-polymerase-dependent increase in signal anywhere in the upstream or early region of *HML**α**1* (Figure 2.1, lanes 2, 3, 4 vs. lane 5). I also did not see a significant increase in reactivity, relative to the signal in naked DNA, in samples treated with nicotinamide (NAM), a chemical inhibitor of silencing, or in samples from a *sir4*Δ mutant (Figure 2.1, lanes 2, 3, 4 vs. lanes 6, 7).

The NAM and *sir4*Δ samples lack Sir-protein repression at *HML**α**1*, but they retain gene-specific Tup1/Ssn6 repression of ***α**1* due to *a1/ **α**2* repression and their pseudo-diploid phenotype (Strathern et al., 1981; Komachi et al., 1994). The pattern of permanganate reactivity was indistinguishable between Sir-protein-repressed copies of *HML**α**1* and copies of *HML**α**1* lacking Sir proteins but repressed by Tup1/Ssn6 acting through the a1/***α**2* repressor, which blocks *a1* transcription in cells expressing both *MATa* and *MAT**α*** or *HMRa* and *HML**α***. Tup1/Ssn6 is a well-studied corepressor-complex that represses transcription by blocking coactivator recruitment (Parnell and Stillman, 2011). The mechanism of repression by *a1/**α**2* through Tup1/Ssn6 does not involve a stalled polymerase and hence the absence of enhanced permanganate reactivity of the *HML**α**1* promoter and early gene region in the *sir4*Δ lane or the lane with material from nicotinamide-treated cells was as expected. The lack of a difference between the permanganate reactivity pattern in Sir-protein-derepressed lanes and in the *SIR4* lane indicated that the mechanism of Sir-mediated repression, like Ssn6-Tup1 repression, operated prior to any engagement by RNA polymerase. In

summation, I find no evidence of DNA melting or a stalled polymerase present at Sir-silenced *HML* **α**1.

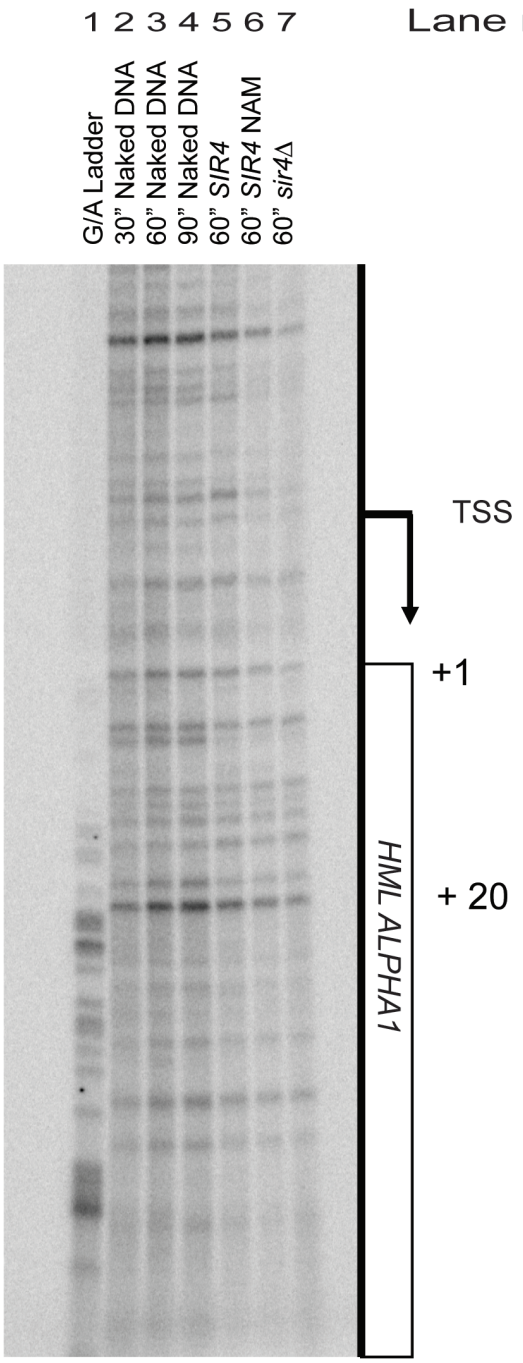


Figure 2.1: The $KMnO_4$ reactivity of *HMLα1 in vivo*
The pattern of $KMnO_4$ reactivity is shown for the promoter and 5' region of *HML**α**1*. Genomic sequences of A+G are shown as a G/A ladder in lane 1. Naked genomic DNA reacted with 20mM $KMnO_4$ for various times are shown in lanes 2-4. The pattern of reactivity for live cells reacted with $KMnO_4$ is shown in lanes 5-7. The reactivity pattern for *SIR4*, *HML**α*** repressed live cells reacted with $KMnO_4$ is shown in lane 6. The pattern of reactivity for cells derepressed with 5mM nicotinamide (lane 6) or genetically by *sir4*Δ (lane 7) are also shown. The arrow denotes the transcription start site as defined by 5' SAGE (Zhang and Dietrich, 2005). The numbers on the right of the panel label bases in *HML**α**1* beginning at the ATG corresponding to positions in the gel.

The recent genome-wide datasets on ChIP-exo-Seq of preinitiation-complexes and nascent transcript sequencing allowed me to determine by independent criteria that, at least for silenced *HML**α**,* that there was no evidence

for RNA polymerase binding or early elongation (Churchman and Weissman, 2012; Rhee and Pugh, 2013), (analysis of published online data).

Sir proteins repressed T7 RNA polymerase at silenced *HMR*

Because I identified that the primary Sir-protein block to transcription occurred before RNA polymerase II melts DNA, I went on to explore how that block might function. The lack of evidence of stalled polymerases in heterochromatin at *HML* was consistent with the steric occlusion model and the preinitiation-complex interference model. Both are based on restricting access of proteins to their target DNA sites to prevent productive transcription from initiating. The difference between the two models hinges on whether the restriction of access affects all proteins with a recognition sequence in the region to a large enough extent to account for the 1000-fold repression observed in silenced chromatin. To date, all tests of the steric occlusion model have been based on the ability of simple DNA-binding proteins with no energy available from nucleotide hydrolysis to access and modify their target site within heterochromatin vs. euchromatin. Restriction enzymes and DNA methylases might not offer an adequate test of the effect of Sir proteins on restricting transcription.

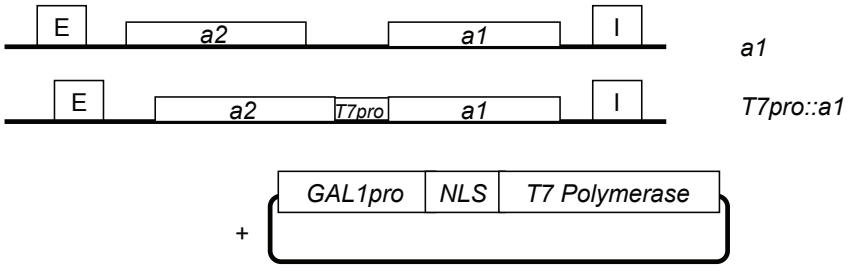
To test the extent that Sir-protein repression can inhibit an RNA polymerase that is not native to yeast and further challenge the steric hindrance model, I designed an assay using a heterologous polymerase normally independent of yeast transcriptional regulation. T7 RNA polymerase consists of a single polypeptide that needs no accessory proteins to transcribe from a T7 promoter in *E. coli* or in eukaryotes (Benton et al., 1990). I replaced the native promoter of *HMRa1* with a minimum optimal T7 promoter (Ujvári and Martin, 1997) (*HMR T7pro::a1*) and expressed T7 RNA polymerase containing a nuclear localization sequence (Figure 2.2a) from the inducible *GAL1* promoter. The *a1* transcript produced by T7 polymerase at *T7pro::a1* would be nearly identical to that expressed from wild-type *HMRa1* in *sir4*Δ cells or from *MATa*. This construction allowed me to use the same qRT-PCR assay to measure silencing of both the native and the engineered *HMR* locus. I tested nuclear-localization-sequence tagged T7 RNA polymerase expressed from a plasmid and from an integrated copy of the gene, and saw no difference on transcript expression of *T7pro::a1* between the two (data not shown). I chose the plasmid-based version due to its versatility for use in further experiments. On a euchromatic template T7 RNA polymerase was able to transcribe *T7pro::a1,* at more than 7 times the level at which *a1* is transcribed from its native promoter in *sir4*Δ cells (Figure 2.2.b, bar 6). T7 RNA polymerase was also specific for the T7 promoter and did not cause a significant increase in *a1* transcription at the wild-type *a1* promoter (Figure 2.2b, bar 4 vs. bar 8). The *T7pro::a1* allele only increased in expression when T7 RNA polymerase was present and expressed (Figure 2.2b, bars 5, 6 vs. bars 1, 2, 9). I observed a background level of *T7pro::a1* expression at approximately 10% the level from a wild-type *HMRa* locus in *sir4*Δ strains lacking

both T7 polymerase and Sir proteins (Figure 2.2b, bars 2, 9). I also observed this background level of transcription in *sir4*Δ strains deleted for the entire promoter region between *a1* and *a2* (data not shown). T7 RNA polymerase was able to transcribe *HMR T7pro::a1* in *SIR4* cells at approximately 40% of the level in *sir4*Δ cells (Figure 2.2b, bar 5).

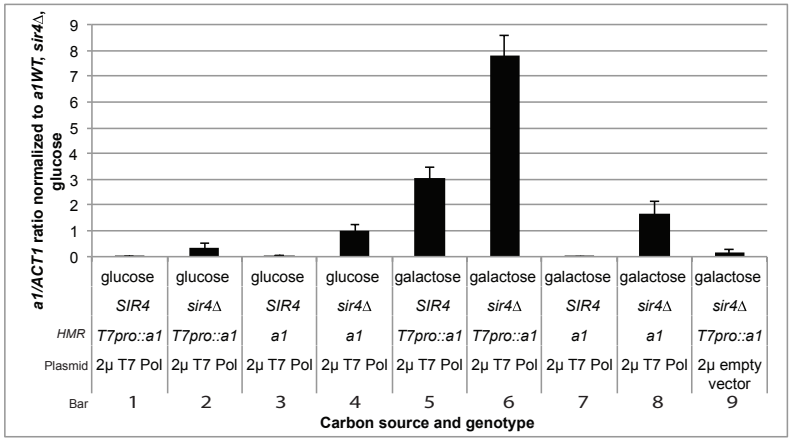
After determining that T7 polymerase was able to transcribe *T7pro::a1,* I investigated if *T7pro::a1* transcripts were 3'-end processed and polyadenylated. I was able to recover *a1* transcripts from both *SIR4* and *sir4*Δ *T7pro::a1* strains transcribed by T7 RNA polymerase that were polyadenylated by using a oligo dT primers during cDNA synthesis. Polyadenylated *T7pro::a1* message was recovered at reduced levels when compared to samples primed using random hexamers as in Figure 2.2. Recovery of *T7pro::a1* cDNA after priming with oligo dT shows that some T7 RNA polymerase-dependent transcripts were 3'-end processed and polyadenylated (data not shown).

Because I determined that *T7pro::a1* transcripts transcribed by T7 RNA polymerase were 3'-end processed, I next sought to determine if they were translated. I created diploid strains in which the only source of *a1* message was at *HMR T7pro::a1*. Sporulation requires a1 protein and can proceed with even small amounts present (reviewed in ((Piekarska et al., 2010)). In my assay only strains that produce a1 protein from *HMR T7pro::a1* would be able to sporulate. I saw zero tetrads from *T7pro::a1* diploids in Spo medium that induces expression of T7 RNA polymerase and contains an excess of nicotinamide, a silencing inhibitor (Figure 2.2c). In contrast I observed a high percentage of tetrads compared to non-sporulating cells in an isogenic diploid strain bearing wild-type *HMRa1* incubated in identical medium. A complete lack of tetrads in derepressed diploids bearing *HMR T7pro::a1* as the only source of *a1* demonstrated that *T7pro::a1* transcripts were not translated into functional a1 protein. Previous work suggests that 5'-transcript capping is defective on some T7 polymerase transcripts in yeast because the secondary structure adopted by certain T7 polymerase-transcripts can interfere the action of 5'-capping proteins, leading to uncapped transcripts (Pinkham et al., 1994; Dower and Rosbash, 2002). If the secondary structure of *T7pro::a1* transcripts resulted in uncapped transcripts that were not translated into a1 protein, that could explain why I failed to recover any tetrads. Additionally, the T7-independent transcription seen in *T7pro::a1 sir4*Δ strains did not lead to translated a1 protein, or successful sporulation, and likely resulted from cryptic transcription initiation within or near *HMR*.

a



b



c

	Sporulation Efficiency Spo medium + galactose, 10mM nicotinamide
*HMLα/HMLΔ, MATα/MATΔ, HMR T7pro::a1/HMR*Δ, *GAL1pro:T7pol*(integrated)	0% (18 days)
HMLα/HMLΔ, MATα/MATΔ, HMR T7pro::a1/HMRa, *GAL1pro:T7pol*(integrated)	40% (4 days)

Figure 2.2: Assays of transcription and translation for *HMR T7pro::a1*
(A) A schematic of *T7pro::a1* at *HMR* in comparison to wild-type *a1*. 20bp of the T7 minimal optimum promoter (Ujvári and Martin, 1997) replaced the region between *a2* and 5bp upstream of *a1* at *HMR*. 5bp upstream of the ATG of *a1* was preserved to optimize potential translation of *T7pro::a1* transcripts. Creation of the*T7pro::a1* alleles was confirmed by sequencing. **(B)** Transcript expression as determined by qRT-PCR of wild-type *a1* and *T7pro::a1* at *HMR* in *SIR4* and *sir4*Δ, with or without expression of T7 RNA polymerase. All *a1* expression values were normalized to *ACT1* and further to the *a1/ACT1* ratio in wild-type *HMRa1*, *sir4*Δ strains grown in glucose. All cultures were seeded from saturated overnight growth in the respective media. cDNA synthesis was primed using random hexamers. Each bar represents 3 biological replicates and error bars depict standard error. **(C)** Genotype and sporulation efficiency of diploid strains used to test for translation of *T7pro::a1* transcripts. Diploids were grown on Spo medium with galactose and 10mM nicotinamide and monitored daily with a hemocytometer to quantify percent of cells sporulated. 3 independent *HMR T7pro::a1* diploids were assayed and no tetrads were seen out of thousands of cells observed.

I next wondered if the kinetic induction of T7 RNA polymerase had an effect on expression of *T7pro::a1* and repression of T7 polymerase due to Sir proteins. I grew cultures in non-inducing medium with raffinose as a carbon source, and induced T7 RNA polymerase expression by adding galactose. The levels of T7 RNA polymerase protein increased over time, reaching a peak by 4 hours, and then gradually declining to steady state levels (Figure 2.3a). To estimate the number of T7 RNA polymerase molecules in the cell, I performed a protein-immunoblot with whole cell extract from cells expressing T7 RNA polymerase and known amounts of purified T7 RNA polymerase protein. I then used a Bradford assay and the molecular weight of T7 RNA polymerase to correlate protein-immunoblot-antibody signal from a known quantity of T7 polymerase protein to the number of T7 polymerase molecules. Using that correlation and the number of cells contained per unit of whole cell extract I was able to estimate that the number of T7 polymerase molecules per cell was on the order of 10,000-20,000 (data not shown). This was roughly equal to the number of active RNA Pol II complexes per cell in previous measurements (Borggrefe et al., 2001).

Having quantitated T7 protein amounts during kinetic induction with galactose, I then investigated *HMR T7pro::a1* transcript levels in the same cultures. T7 RNA polymerase robustly transcribed *T7pro::a1* transcripts over time (Figure 2.3b, *sir4*Δ). In contrast to transcription in the *sir4*Δ mutant grown in galactose medium alone, T7 RNA polymerase was dramatically repressed by Sir proteins when induced in *SIR4* strains (Figure 2.3b). Expression at early time points (t=2 hours) was 200-fold less than in the *sir4*Δ mutant. Sir proteins were able to repress T7 transcription 200-fold. The extent of repression was reduced at later time points, as evidenced by low levels of *a1* transcript from *T7pro::a1* in *SIR4* cells. To further investigate *T7pro::a1* transcription by T7 polymerase in *SIR4* strains, I performed an additional identical experiment in *SIR4* cells and tracked *a1* expression over a longer time period. I detected a consistent increase in *T7pro::a1* transcripts over time (Figure 2.3c). Additionally, when cells were assayed after entering stationary phase, *a1* expression levels increased (data not shown), similar to (Figure 2.2b bar 5).

Interpretation of previous experiments had been limited by the lack of knowledge of whether transcription per se might affect nucleosome formation and the stability of Sir-protein association with nucleosomes. Therefore, I tested whether Sir proteins remain associated with *HMR* in cells with T7 polymerase transcribing from *T7pro::a1*. Sir-protein enrichment, as measured by ChIP in the same cultures as Figure 2.3c, remained constant at two regions within the *a1* gene and at the two silencers of *HMR* (Figure 2.4), even as a1 transcript levels increased (Figure 2.3b). However, the issue of what happens to Sir proteins at *HMR* at later time points when RNA transcripts were detected is not fully resolved. The ChIP assay I performed cannot determine if precipitated DNA fragments associated with Sir proteins were recovered from cells undergoing

active T7 transcription or not. Therefore, I could not exclude the possibility that the cells that produced the *a1* transcripts were a different subset of the culture from the cells that contributed the ChIP signal of Sir proteins at *HMR*. It remained possible that T7 polymerase transcription of a Sir+ template was able to evict Sir proteins.

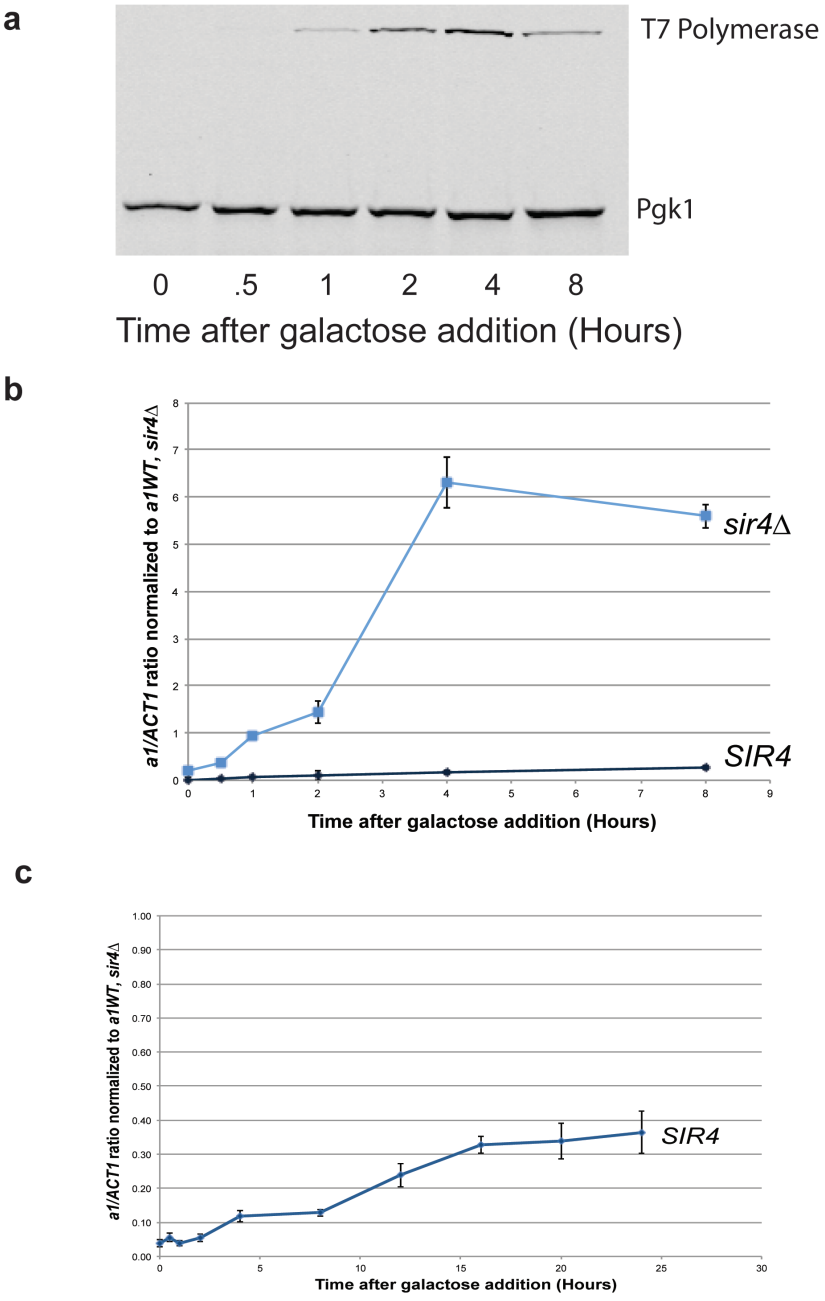


Figure 2.3: Transcript analysis of *HMR T7pro::a1* upon kinetic induction of T7 RNA polymerase in *SIR4* and *sir4*Δ strains

(A) T7 RNA polymerase proteins levels before and upon galactose induction in CSM-leu media. Pgk1 levels are shown as a loading control. **(B)** *a1* transcript expression of *T7pro::a1* as determined by qRT-PCR in *SIR4* and *sir4*Δ strains upon kinetic induction of T7 RNA polymerase

and media switch from raffinose to galactose. All *a1* expression values were normalized to *ACT1* and further to the *a1/ACT1* ratio in wild-type *HMRa1 sir4*Δ strains. Each point represents 3 biological replicates and error bars depict standard error. **(C)** *a1* transcript expression of *T7pro::a1* as determined by qRT-PCR in *SIR4* cells over an extended time course upon kinetic induction of T7 RNA polymerase and a media switch to galactose. All *a1* expression values were normalized to *ACT1* and further to the *a1/ACT1* ratio in wild-type *HMRa1 sir4*Δ strains. Each point represents 3 biological replicates and error bars depict standard error.

At later time points I detected low-level expression of *a1* transcripts from the *T7pro::a1* in *SIR4* cells (Figure 2.3b, 2.4). This low-level expression may have resulted from adventitious binding of the T7 promoter, given the vast excess of T7 polymerase, perhaps occurring during replication of the *HMR* locus or other disruptions of chromatin structure concurrent with the cell cycle or stationary phase.

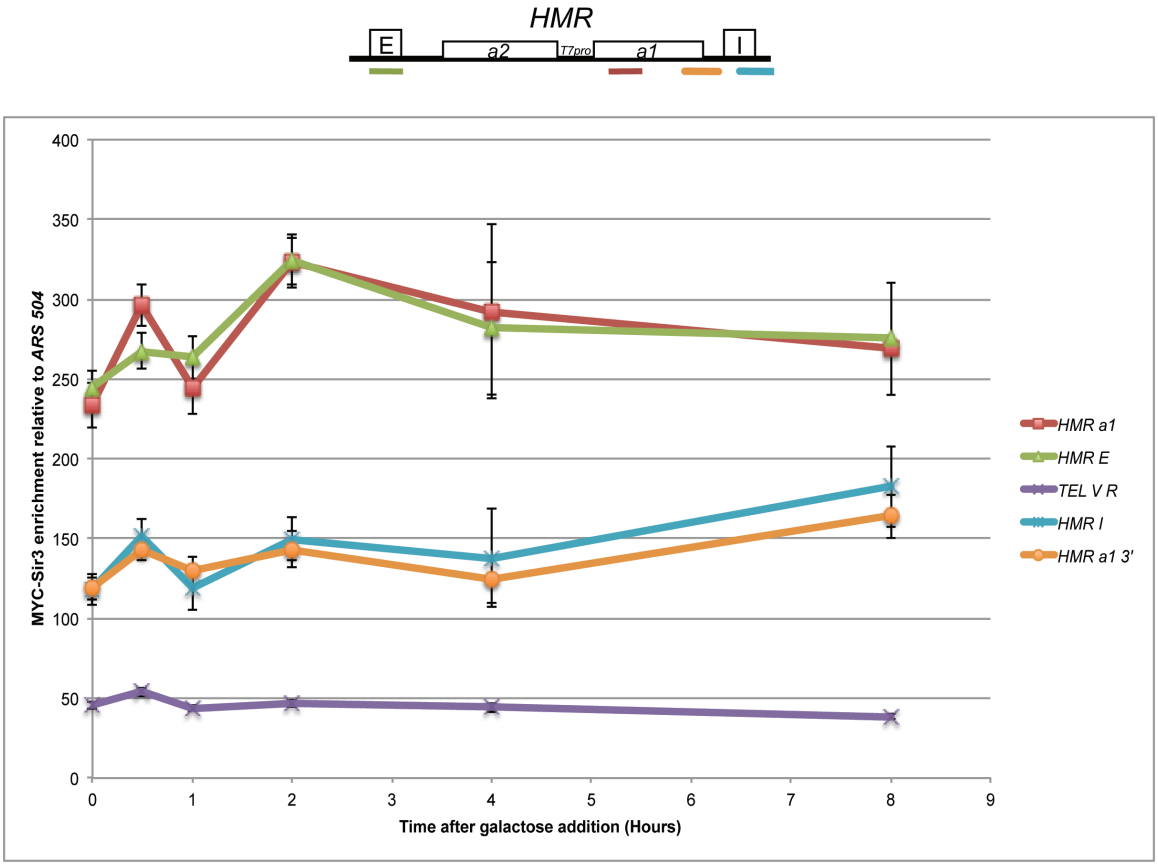


Figure 2.4: 13xMYC-Sir3 enrichment at *HMR* and telomere V R upon kinetic induction of T7 RNA polymerase in *SIR4* strains
13xMYC-Sir3 enrichment as assayed by Sir3 ChIP followed by qRT-PCR at *HMR* and telomere V R from the same *SIR4* kinetic cultures described in Figure 2.3. Values are displayed as 13xMYC-Sir3 enrichment relative to an *ARS504* negative control primer set. The cartoon above the plot shows the location of the primers sets at *HMR*. Each point represents 3 biological replicates, except the *HMRa1* 8-hour time point, which is an average of 2 biological replicates. Error bars depict standard error.

It also remained a possibility that the sequence manipulation of *HMRa* to generate *HMR T7pro::a1* could have disrupted a necessary sequence-based quality of the locus or promoter that affected nucleosome formation or position and hence, Sir protein occupation of an important promoter or site. Therefore, I examined the distribution of Sir proteins and by inference, nucleosomes, across *HMR T7pro::a1* in a silenced strain in the absence of T7 transcription. In collaboration with a colleague in the lab we performed ChIP-Seq of Sir3 in *HMR T7pro::a1* strains lacking T7 RNA polymerase. We detected high levels of Sir3 enrichment throughout *HMR* and that saw the T7 promoter and *a1* gene body was covered by Sir proteins (Figure 2.5). Because Sir3 binds nucleosomes I could also infer that the promoter and gene body was covered by nucleosomes. This verified that the repression of *HMR T7pro::a1* due to Sir proteins was consistent with their position throughout *HMR* and not due to an obvious nucleosome or Sir-protein mislocalization defect. Together all of these results demonstrate that Sir proteins were a significant barrier to transcription by T7 RNA polymerase.

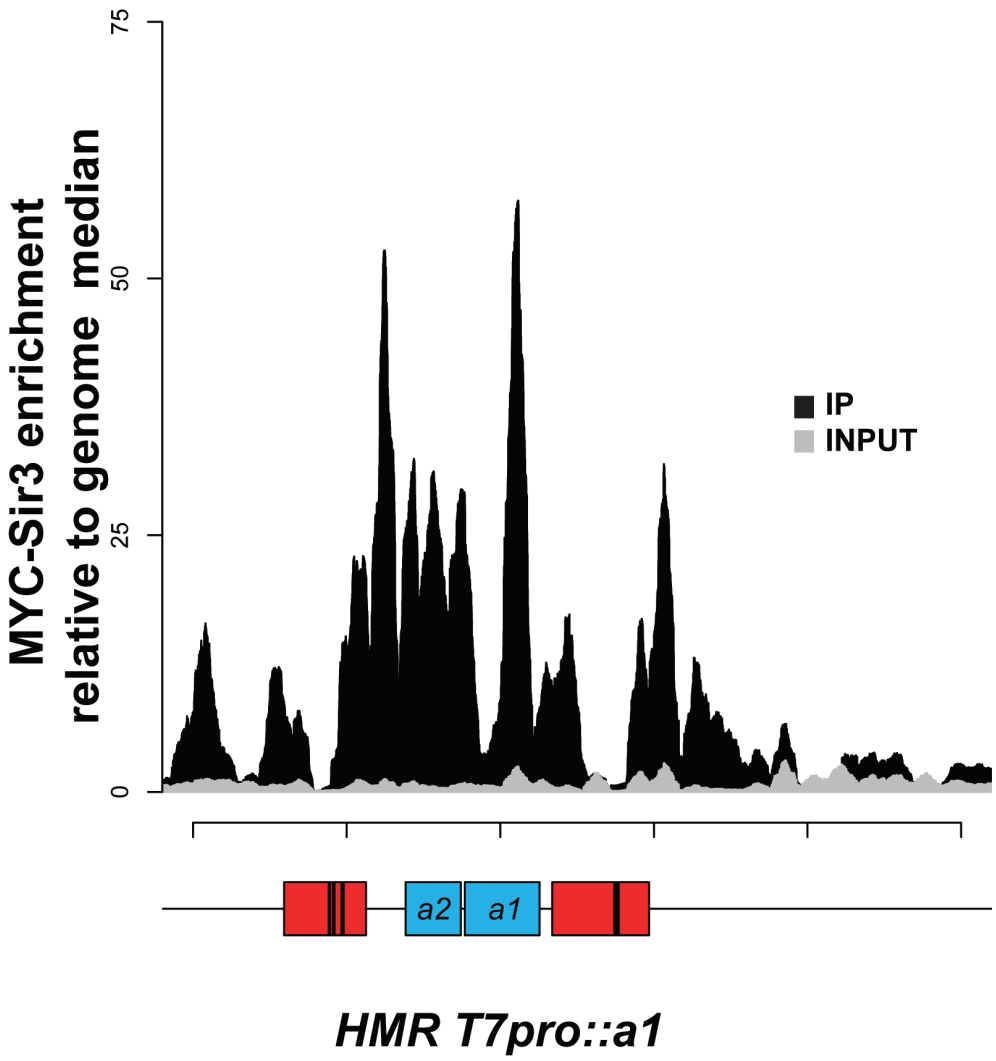


Figure 2.5: 13XMYC-Sir3 enrichment at *HMR T7pro::a1* lacking T7 RNA polymerase as assayed by ChIP followed by high-throughput sequencing
13XMYC-Sir3 enrichment was measured by ChIP followed by high throughput sequencing at *T7pro::a1* in a *SIR4* strain lacking T7 RNA polymerase. IP and Input signals are plotted relative to the genome median. The diagram below the graph depicts position of the reads relative to features at *HMR T7pro::a1*. Red boxes depict silencer sequences and black lines the specific silencer DNA-binding sites.

The Gal4 activator was largely insensitive to Sir-protein silencing

Yeast genes vary with respect to their sensitivity to silencing when placed at *HML* or *HMR*. I hypothesized that the sensitivity of a gene to Sir-based silencing might reflect some quality of the particular transcriptional activator acting at that gene. To test this idea, I replaced the promoter of *HMRa1* with the full 450 bp *GAL1* promoter (*HMR GAL1pro::a1*), maintaining the approximate size of the *HMR* locus and the distance from the promoter to silencers (Figure 2.6a). I then assayed expression of *HMR GAL1pro::a1* in cells grown under repressing, non-inducing and inducing conditions (Figure 2.6b). As expected, in

SIR4 and *sir4*Δ strains *HMR GAL1pro::a1* was not expressed in repressing or non-inducing conditions (Figure 2.6, bar 1, 2, 4, 5). Again, as expected *GAL1pro::a1* was expressed in *sir4*Δ strains grown in inducing, galactose-containing media (Figure 2.6b, bar 6). In addition, *GAL1pro::a1* expression in *SIR4* strains grown in inducing, galactose medium was 60% of the level of the *sir4*Δ strain (Figure 2.6b, bar 3). These results verified that *GAL1pro::a1* was expressed and largely able to escape Sir-protein repression.

I expected *HMR GAL1pro::a1* transcripts to be translated, as the *GAL1* promoter has been successfully used to drive expression of many yeast genes. To verify that was the case for *GAL1pro::a1* specifically, I tested if *GAL1pro::a1* transcripts were translated using a patch mating assay that required functional a1 protein to achieve mating. This assay also allowed me to determine if galactose repression could compensate for Sir-protein repression and repress *HMR* in the absence of Sir proteins at *HMR*. I found *GAL1pro::a1* was translated because *MAT**α**, HMR GAL1pro::a1, sir4*Δ strains did not mate when grown on galactose medium (Figure 2.6c, line 2 galactose). I also saw a reduction in mating efficiency in *MAT**α**, HMR GAL1pro::a1, SIR4* strains, indicating reduced expression of *HMR GAL1pro::a1* in the presence of Sir proteins (Figure 2.6c, line 1 galactose). Reduced mating efficiency in *SIR4* strains assayed on galactose medium supported the RNA phenotype presented in Figure 2.6b and demonstrated the expression level *HMR GAL1pro::a1* in *SIR4* cells was physiologically relevant since it functionally decreased mating efficiency. Also, galactose repression compensated for the loss of Sir-protein repression by suppressing the non-mating phenotype of a *sir4*Δ and repressing *HMR GAL1pro::a1* in *sir4*Δ strains grown in dextrose medium (Figure 2.6c, line 2 dextrose vs. galactose).

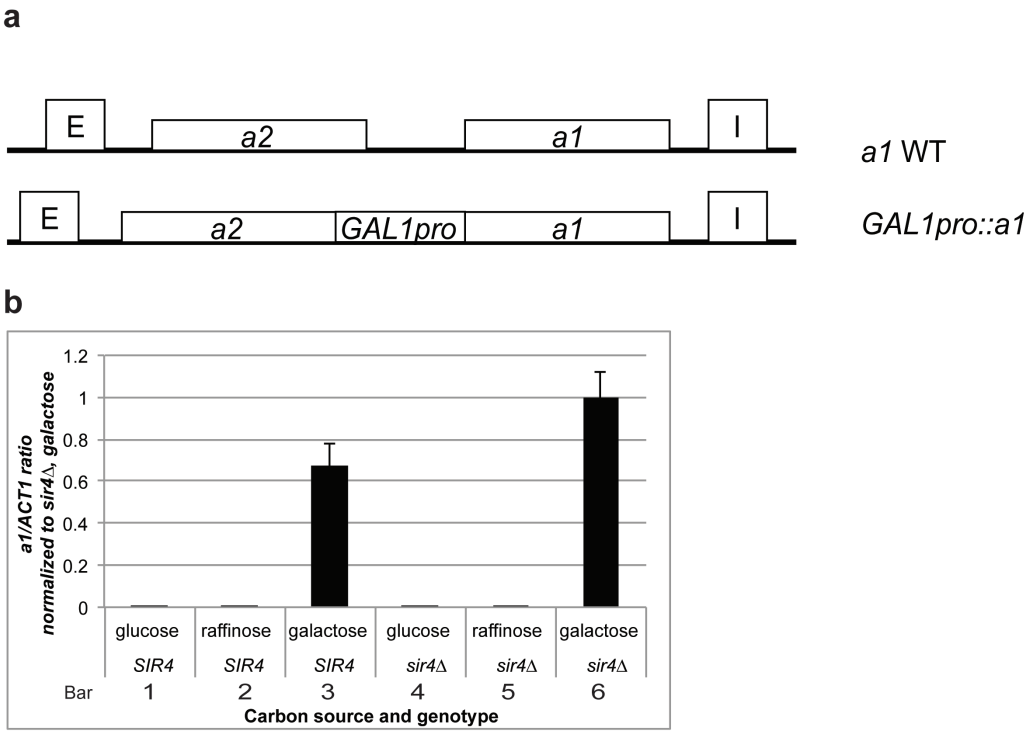


Figure 2.6: Assays of transcription and translation for *HMR GAL1pro::a1*
(A) A schematic of *GAL1pro::a1* at *HMR* in comparison to wild-type *a1*. 450bp of the *GAL1* promoter containing 4 UAS_g sites replaced the region between *a2* and *a1* at *HMR*. Creation of the *GAL1pro::a1* allele was confirmed by sequencing. **(B)** mRNA expression as determined by qRT-PCR of wild-type *a1* and *GAL1proL::a1* at *HMR* in *SIR4* and *sir4*Δ strains on various carbon sources. All *a1* expression values were normalized to *ACT1* and further to the *a1/ACT1* ratio in *GAL1pro::a1*, *sir4*Δ, strains grown in galactose media. Each bar represents 3 biological replicates and error bars depict standard error. **(C)** Patch mating assay between various *HMR GAL1pro::a1* or *HMR a1* strains on dextrose or galactose media. Query strains were mated to tester strains prototrophic for all markers expect for *his4* and any resulting diploids were replica plated onto minimal medium containing dextrose or galactose. Growth of diploids on minimal media demonstrated the ability to mate.

Because kinetic analysis of *T7pro::a1* expression yielded important insights into repression by Sir proteins, I performed a similar set of experiments using *HMR GAL1pro::a1* strains. I grew cultures in non-inducing raffinose media, induced expression of *GAL1pro::a1* by adding galactose (t=0),and monitored expression of *GAL1pro::a1* mRNA over time. In the first hour after galactose induction I saw was no difference in transcription from *HMR GAL1pro::a1* between *sir4*Δ and *SIR4* strains (Figure 2.7). After two hours, *sir4*Δ strains showed increased *a1* mRNA levels relative to *SIR4* strains (Figure 2.7). Expression of *HMR GAL1pro::a1* was approximately 1.5-2-fold greater in *sir4*Δ compared to *SIR4* strains at all time points after 1 hour. *SIR4, GAL1pro::a1* strains displayed transcript levels approximately equal to wild-type *HMRa1 sir4*Δ strains, showing that the magnitude of silencing escape of the *GAL1pro::a1* allele reached physiologically meaningful levels.

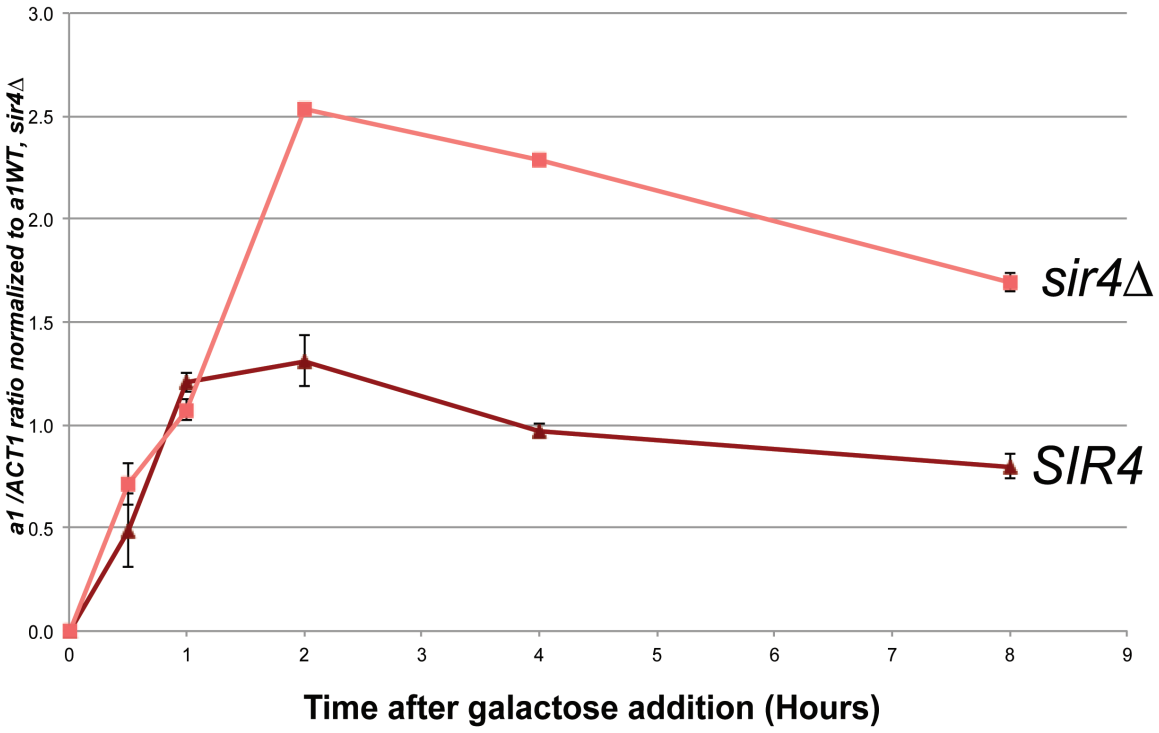


Figure 2.7: mRNA analysis of *HMR GAL1pro::a1* upon kinetic induction of T7 polymerase in *SIR4* and *sir4*Δ strains
a1 mRNA expression of *GAL1pro::a1* as determined by qRT-PCR in *SIR4* and *sir4*Δ strains upon kinetic induction of T7 polymerase with galactose. Strains were grown initially in CSM raffinose media and galactose was added to induce the galactose transcriptional response. All *a1* expression values were normalized to *ACT1* and further to the *a1/ACT1* ratio in wild-type *HMRa1*, *sir4*Δ strains. Each point represents 3 biological replicates and error bars depict standard error.

Because T7 polymerase did not appear to displace Sir proteins during transcription when assayed by ChIP, I wondered if the substantial RNA Pol II transcription driven by the GAL1 promoter on a Sir-protein bound template would displace Sir proteins at *HMR*. To answer this question, I monitored Sir3 enrichment by ChIP in the same *SIR4* cultures as above. Sir-protein enrichment

at the *GAL1* promoter at *HMR*, an internal region of *a1*, and at *HMR-E* significantly decreased between t=0 and t=2 hours (paired students t-test p=.012, p=.009, p=.021 respectively) (Figure 2.8a). This result demonstrated that RNA Pol II was able to displace Sir proteins during transcription in *SIR4* cells. However, in *SIR4* strains that showed expression of *HMR GAL1pro::a1*, Sir-protein occupancy was reduced but not eliminated (Figure 2.8a), suggesting Sir proteins had been incompletely removed or were still attempting to bind and silence an actively transcribed locus.

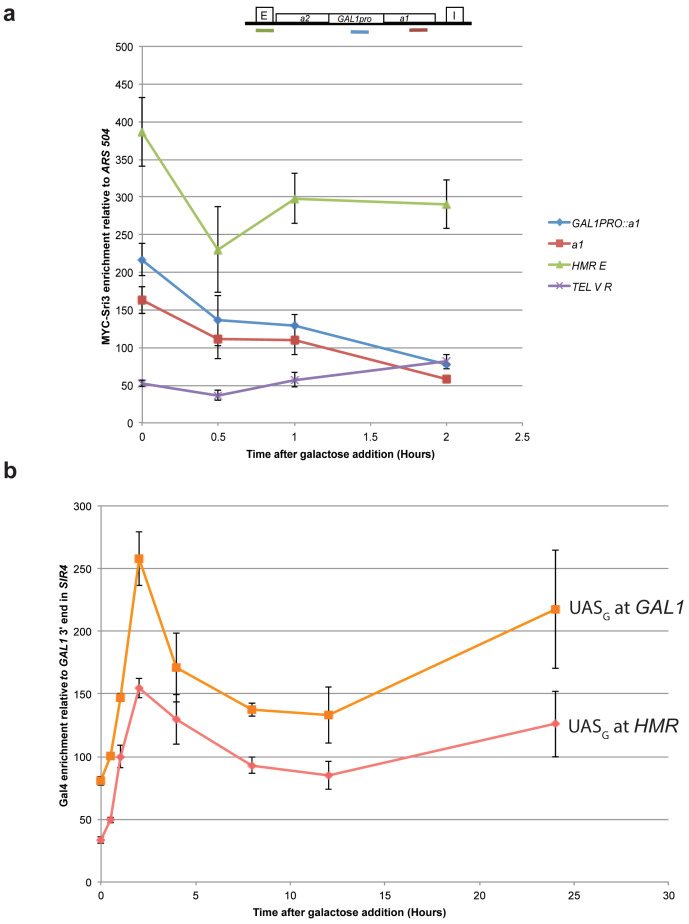


Figure 2.8: 13xMYC-Sir3 and Gal4 enrichment at *HMR GAL1pro::a1* upon kinetic galactose induction in *SIR4* strains
(A) 13xMYC-Sir3 enrichment as assayed by Sir3 ChIP followed by qRT-PCR at *HMR* from the same *SIR4* kinetic cultures described in Figure 2.7. Values are displayed as 13xMYC-Sir3 enrichment relative to an *ARS504* negative control primer set. All HMR primer sets show a statistically significant reduction in Sir3 occupancy between 0 and 2 hours (see text for p-values). The cartoon above the plot shows the location of the primers sets at *HMR*. Each point represents 3 biological replicates. Error bars depict standard error. **(B)** Gal4 enrichment as assayed by Gal4 ChIP followed by qRT-PCR at *HMR* and *GAL1* from the same *SIR4* kinetic cultures described in Figure 2.7. Values are displayed as Gal4 enrichment relative to a *GAL1 3'*-intrergenic region negative control primer set. Each point represents 3 biological replicates. Error bars depict standard error.

Because RNA polymerase was able to access its target within silenced *HMR GAL1pro::a1* and perform transcription, I wanted to determine to what extent the Gal4 activator was able to access its template in silenced chromatin. The identical transcript induction kinetics in *SIR4* and *sir4*Δ strains over the first hour suggested that Gal4 had already bound the Gal4 binding site in cells of either genotype before induction began. To answer this question definitively, I performed Gal4 ChIP in *SIR4* and *sir4*Δ strains at *HMR* and at the native *GAL1* locus. In *SIR4* strains, Gal4 was able to bind its upstream activating sequence within silenced chromatin both before and after galactose induction (Figure 2.8b). Upon induction, Gal4 enrichment levels increased at both *HMR GAL1pro::a1* and at the native *GAL1* locus (Figure 2.8b). However Gal4 showed lower enrichment at *HMR* relative to the same sequence at the native *GAL1* locus (Figure 2.8b). This suggests that either the *GAL1* promoter at *HMR GAL1pro::a1* did not recruit or bind Gal4 with the same affinity as the wild-type *GAL1* promoter at the native *GAL1* locus, or that Sir proteins reduced Gal4 binding in silenced chromatin. To resolve that question, I compared the enrichment of Gal4 at *HMR* vs. the native *GAL1* locus in *SIR4* and *sir4*Δ cells. I found the pattern of Gal4 enrichment in *sir4*Δ strains was similar to *SIR4* strains, both before and in response to induction (Figure 2.9). Gal4 enrichment at *HMR* was always lower relative to native *GAL1* (Figure 2.8, 2.9). However, when I compared the ratio of Gal4 enrichment at *HMR GAL1pro::a1/GAL1* in *SIR4* and *sir4*Δ strains I observed that Sir proteins did not significantly reduce the occupancy of Gal4 at *HMR GAL1pro::a1* at any time point tested (Figure 2.9). This shows that Gal4 bound the *GAL1* promoter at *HMR* more poorly than the native *GAL1* locus and that Sir proteins do not significantly reduce the ability of Gal4 to bind its target activating sequence in silenced chromatin.

Because I had identified the Gal4 activator was able to escape repression due to silencing, I wanted to determine if decreasing Gal4 activation strength would compromise its ability to escape silencing. Therefore, I created a point mutant in the central domain of Gal4 (gal4L331P) that is reported to compromise its ability to activate transcription but not to bind DNA (Johnston and Dover, 1988; Mylin et al., 1990). I then assayed the ability of the gal4L331P allele to escape Sir-protein repression by measuring mRNA in *SIR4* and *sir4*Δ strains. In comparison to wild-type Gal4, gal4L331P showed reduced ability to activate transcription of *HMR GAL1pro::a1* in *sir4*Δ strains (Figure 2.10, note the y-axis scale). Sir proteins further reduced *a1* transcript levels activated by gal4L331P at *HMR GAL1pro::a1* in *SIR4* (Figure 2.10, right panel). Repression by Sir proteins at *GAL1pro::a1* activated by wild-type Gal4 was roughly 2-fold, however repression by Sir proteins of *GAL1pro::a1* activated by gal4L331P increased to 12-fold. Thus, decreasing the ability of an activator to activate transcription increases silencing efficiency. Overall I find the Gal4 activator is largely insensitive to Sir-based silencing and can promote transcription at the *GAL1* promoter even when it is repressed by Sir proteins. In addition, compromising the ability of the Gal4 activator to activate transcription increases silencing efficiency.

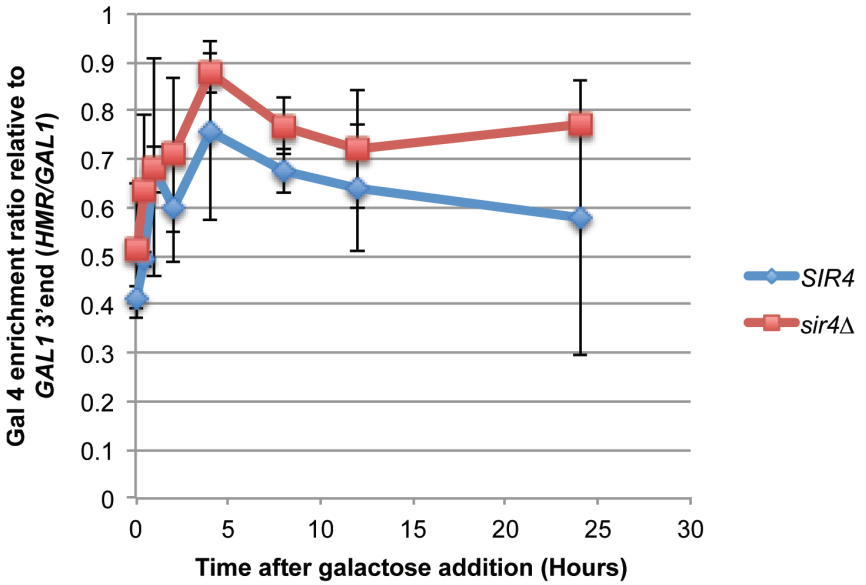


Figure 2.9: Gal4 enrichment at *HMR GAL1pro::a1* and *GAL1* upon kinetic galactose induction in *SIR4* and *sir4*Δ strains
13xMYC-Sir3 enrichment as assayed by Sir3 ChIP followed by qRT-PCR at *HMR* from the same *SIR4* and *sir4*Δ kinetic cultures described in Figure 2.7. Values are displayed as the ratio of Gal4 enrichment at *HMR GAL1pro::a1* relative to *GAL1* and a *GAL1* intrergenic region negative control primer set to account for the reduced ability of *HMR GAL1pro::a1* to recruit Gal4 compared to the native *GAL1* locus. Each point represents 3 biological replicates. Error bars depict standard error.

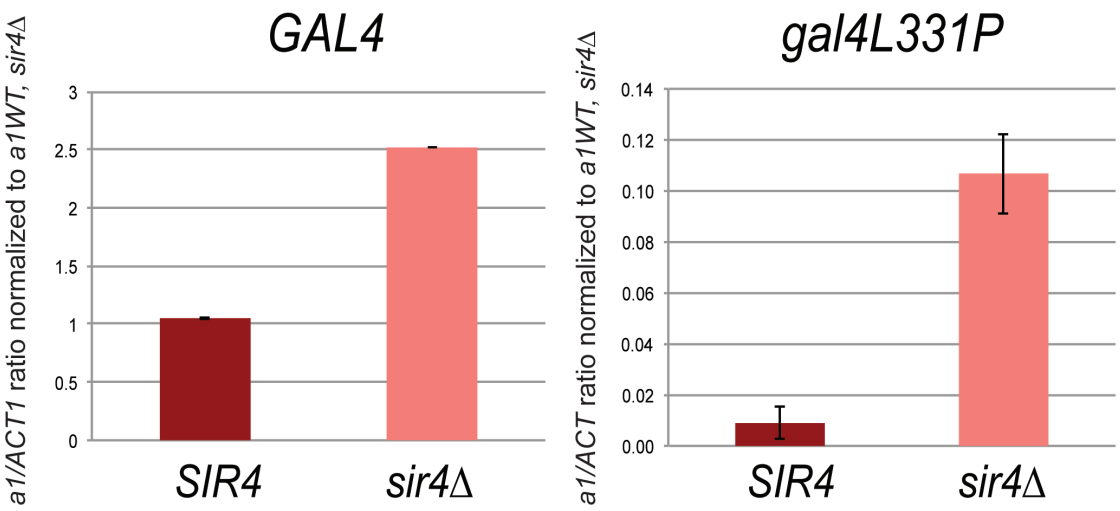


Figure 2.10: mRNA analysis of Gal4 wild-type and gal4L331P and effects on transcriptional activation and silencing at *HMR GAL1pro::a1*
mRNA expression as determined by qRT-PCR of Gal4 wild-type and gal4L331P mutant strains bearing *GAL1pro::a1* at *HMR* in *SIR4 and sir4*Δ strains in galactose media. All *a1* expression values were normalized to *ACT1* and further to the *a1/ACT1* ratio in *a1 wild-type*, *sir4*Δ, strains grown in galactose media. Each bar represents 3 biological replicates and error bars depict standard error.

Discussion:

The primary mechanism of transcriptional repression does not operate through a paused polymerase

My results directly refuted the downstream-inhibition model for transcriptional silencing in yeast, and call into question the data supporting it. The downstream-inhibition model necessarily predicts that RNA Pol II is found within Sir-silenced heterochromatin in a DNA melted state, bound on the template, and with the two strands of the template held apart in what is known as a stalled transcription bubble. I found no evidence of stalled polymerase present at *HMLα1* in silenced cells. Analysis of recent ChIP-exo-Seq (Rhee and Pugh, 2013) and nascent transcript-Seq (Churchman and Weissman, 2012) datasets confirmed that RNA PolI II was absent from silenced *HML*.

It formally remains possible that Sir proteins repress *HMR* using a stalled polymerase mechanism but I find that to be highly unlikely given that identical composition of the Sir-protein complex present at both *HML* and *HMR* and the similar behavior of both loci in numerous transcriptional silencing assays. My data also allowed the possibility that Sir proteins could repress transcription after RNA Pol II binding at some level during the elongation process, but this could not be the primary mechanism and would need to be a distributed effect throughout the locus to elude detection by the permanganate-reactivity assay. *In vitro*, Sir proteins can inhibit elongation on reconstituted, Sir-protein-coated, chromatinized, linear-DNA fragments that have RNA Pol II and a complete transcription complex assembled on them (Johnson et al., 2009; 2013). My *in vivo* data showed elongation does not occur at a detectable or phenotypically meaningful level at *HML* and thus, inhibition of elongation was not a primary mechanism of silencing.

The lack of a stalled RNA Pol II in silenced chromatin required that the primary repressive mechanism of Sir-protein-mediated silencing acts before DNA melting in the transcription cascade. Even if some small fraction of cells do have a stalled polymerase that escaped detection by the permanganate assay, it is not possible that mechanism could account for silencing in the majority of cells and the 1000-fold repression of *HML* in wild-type cells. Previous reports of ChIP (Gao and Gross 2008) and ChIP-genome-wide array data (Steinmetz et al., 2006) that inspired the downstream-inhibition model were likely misled by the relative shearing resistance of silenced chromatin (Teytelman et al. 2009) resulting in artifactual precipitation of *HML* and *HMR* with RNA polymerase on inadequately sheared chromatin.

Molecular mechanisms of transcriptional silencing

The T7 polymerase assay described here represented, to the best of my knowledge, the best and most stringent test of the steric occlusion model for several reasons: it is the first test of the steric occlusion model that used a transcription protein rather than a simple DNA binding protein, as a quantitative test of the Sir-protein transcriptional repression mechanism. Also, the assay provides a strong challenge to Sir-protein repression. Within 2 hours of induction, the level of T7 polymerase was comparable to the level of RNA Polymerase II. But, these cells had only a single T7 promoter, in contrast to thousands of targets for RNA Pol II. Therefore the T7 polymerase transcription assay stringently measured effectiveness of steric occlusion as a silencing mechanism. Sir-based silencing was a significant impediment to T7 polymerase transcription. The repression due to Sir proteins on T7-mediated transcription of *HMR T7pro::a1* in *SIR4* versus *sir4*Δ cells was 200-fold at 2 hours after induction, though somewhat lower at longer time points. Quantitatively, 200-fold repression was only a 5-fold effect away from equaling the 1000-fold magnitude of repression of RNA Pol II by Sir proteins at *HMRa1*.

My data demonstrated that the mechanism of Sir-based silencing was largely independent of any special feature of the native transcription machinery. Occlusion of a specific eukaryotic transcription factor or co-activator would have no effect on blocking transcription by T7 RNA polymerase, yet T7 polymerase transcription from the T7 promoter was still dramatically repressed.

It remains unclear if T7 RNA polymerase was physically prevented from binding its promoter in silenced chromatin, or if the 200-fold difference in repression between *SIR4* and *sir4*Δ strains reflects a mixture of reduced polymerase binding, and inhibition of initiation and/or elongation. T7 RNA polymerase has so far been difficult to ChIP in yeast, but a difference in T7 RNA polymerase occupancy between Sir+ and Sir- cells would provide an answer. Future experiments utilizing T7 RNA polymerase mutants that are competent for promoter binding but not elongation could also differentiate between repression due to reduced binding or inhibited elongation. It is also possible that the difference between the 200-fold repression of T7 transcription versus the 1000-fold repression of Pol II reflects a higher affinity of T7 polymerase for its promoter, or the higher processivity of T7 polymerase (Ujvári and Martin, 1997).

Addressing a further case of the steric occlusion model, I demonstrated the Gal4 activator (99 kDa), of similar size to T7 RNA polymerase (100 kDa), was able to bind it recognition sequence in heterochromatin and activate transcription, regardless of the presence or absence of Sir proteins, whereas T7 polymerase largely could not transcribe a Sir+ template. So, the difference in Sir-protein repression of Gal4 versus T7 polymerase could not simply reflect a difference in activating or transcribing molecule size.

The observed 2-fold repression of transcription in *SIR4 GAL1pro::a1* strains demonstrated it was likely that sterics and/or inhibition of elongation by Sir

proteins had some contribution to repression, but 2-fold repression alone cannot explain the 1000-fold repression of *HMR* relative to *MAT*. Binding of Gal4 to *GAL1pro::a1* was indistinguishable in *SIR4* and *sir4*Δ cells, so activator occlusion or interference cannot explain silencing in the case of Gal4. Indeed it appears that the specific activator being silenced or activator affinity or strength itself may be a factor in determining the efficiency of silencing in yeast. My data are compatible with a model for silencing where activators and the Sir proteins are engaged in a dynamic affinity-based competition for binding sites at the promoter of silenced genes. To bind and activate transcription, activators would need to have higher affinity for their promoters than that of the Sir proteins for the nucleosomes surrounding the necessary sites for activation; activators with an affinity for their binding sites lower than that of the Sir proteins for the nucleosomes surrounding the sites required for activation would not be able to bind and therefore transcription would be silenced. This would impose a threshold for activation or silencing based on the affinity of the Sir proteins for activation sites within the promoters of silenced genes. My data showed the *GAL1* promoter/Gal4 activator pair was above this threshold. In support of this model, the incomplete removal of Sir proteins from *Gal1pro::a1* in *SIR4* cells even as transcript levels reached their maximum suggested that Sir proteins may have been attempting to bind and silence *GAL1pro::a1* despite active transcription through the locus.

Implications on the mechanism(s) of silencing at *HMR* and *HML*

The affinities of Abf1, (the activator for *a1* at *MAT* and *HMR* (McBroom and Sadowski, 1995)) Gal4, and T7 polymerase for their binding sites appear to be similar, in the low nM range (Taylor et al., 1991; Ujvári and Martin, 1997; Beinoravičiūtė-Kellner et al., 2005). Yet, T7 RNA Polymerase and Abf1-dependent transcription is dramatically repressed, but Gal4 both has access to its binding site and can promote transcription in the presence of Sir proteins. However, those affinities were measured *in vitro* and it is possible that the *in vivo* affinities for a dynamic chromatin template are substantially different. In addition, binding of Gal4 to DNA is cooperative (Giniger and Ptashne, 1988) and that cooperativity may enhance the ability of Gal4 to bind its target in silenced chromatin, in comparison to T7 RNA polymerase. My results demonstrated that Gal4 was able to recruit productive transcription complexes to silenced regions *in vivo*. This contradicts previous *in vitro* data claiming activator-interference is a primary silencing mechanism responsible for silencing a Gal4 activator (Johnson et al., 2013). The dynamic affinity-based competition model also makes the prediction that native promoters and activators at *HML* and *HMR* have an affinity for each other below that of the Sir proteins for their binding sites leading *HML* and *HMR* to become silenced.

Little is known about the status of activators at silenced promoters at *HML* and *HMR*. It remains possible that Abf1 is prohibited from accessing its target sequence specifically in the promoter of *HMR* in Sir+ cells. Previous genome-

wide analyses have often been unable to provide data on Abf1 at *HMR* or Rap1 at *HML*, because sequences in common between *HML*, *MAT,* and *HMR* precluded unambiguous analysis. Based on the position of the Abf1 binding site at *HMR*, it was difficult to conclusively recover epitope-tagged Abf1 binding by ChIP, likely because of the shearing resistance of silenced chromatin (Teytelman et al., 2009) and the effects of crosslinking on recovery of specific regions at *HML* and *HMR* by ChIP (Thurtle and Rine, 2013 submitted). It will require further efforts to conclusively determine if native activators for *HML* and *HMR* are present at their binding sites within silent chromatin.

The dynamic affinity-based competition model for transcriptional silencing supported by my data also suggests that there is nothing intrinsic to the genes at *HML* and *HMR* preventing them from being expressed besides their specific promoter/activator combinations. Manipulations that increase the local concentration of activators relative to Sir proteins, such as activator tethering or mutations in DNA or protein sequence that increase the affinity of specific activators for their binding sites within silenced chromatin, would have the effect of decreasing the efficiency of silencing and allowing expression of normally silenced genes.

The interplay of transcription activation strength and silencing

It is known that promoter strength influences the S phase requirement for the establishment of silencing (Ren et al., 2010). The *HMLα1* promoter has a lower absolute expression level, and is weaker than the *HMRa1* promoter when both are assayed in the euchromatin state (Ren et al., 2010). In silencing establishment assays, *HMLα* does not require passage through the cell cycle to become silenced, while *HMRa* does (Ren et al., 2010). In addition, I demonstrated that a weakened gal4L331P allele had a reduced ability to activate transcription of *GAL1pro::a1* in *sir4*Δ samples, and increased the efficiency of silencing in *SIR4* samples. Even though this mutant is reported to be compromised for transcriptional activation and not DNA binding (Mylin et al., 1990), later work shows that activation-domain strength can affect the occupancy of transcriptional activators at promoters (Bunker and Kingston, 1996; Tanaka, 1996). It is possible that the activation deficient gal4L331P allele also had reduced affinity for or occupancy at its binding site, and that is what lead to its increased ability to be silenced.

Finally, in cases where I showed that the Gal4 activator was able to access its binding site within silenced chromatin, transcription was still repressed 1.5-2 fold. 2-fold repression of a promoter that escapes the majority of Sir-protein silencing suggests that regardless of any other promoter/activator affinity-based mechanism, steric hindrance by Sir proteins also inhibits transcription as well. It is likely that the mechanism of Sir-protein silencing represents the quantitative addition of multiple repressive factors: most importantly, a dynamic affinity-based completion for binding site and activation between Sir proteins and

activators, but also a general steric inhibition reducing the binding of multiple individual factors required for transcription, and inhibition of transcriptional elongation efficiency. These factors could coordinate to accomplish the 1000-fold reduction in transcript levels seen at wild-type silenced loci.

Broader implications of these results

The mechanism of Sir-protein silencing may be specific to *Saccharomyces cerevisiae* and its close relatives because the specific suite of proteins required to establish and maintain silencing are specific to, and even within parts of, the *Saccharomyces* clade (reviewed in (Hickman et al., 2011)). Perhaps unsurprisingly, in contrast to my results, studies using Gal4 and T7 polymerase to investigate *Drosophila* Polycomb repression report that Polycomb blocks Gal4, but not T7 polymerase from productive transcription in flies (McCall and Bender, 1996; Fitzgerald and Bender, 2001).

Potassium permanganate assays have previously been used to identify open promoter complexes associated with inducible transcription in yeast (Giardina and Lis, 1993), and developmentally-regulated paused polymerases in flies (Zeitlinger et al., 2007). Post-RNA Pol II binding-regulation is seen in stationary phase in yeast (Radonjic et al., 2005), so it was reasonable to suppose that polymerase stalling could have been the mechanism by which Sir proteins restricted transcription. My data refuted this supposition. Groups have assayed for stalled or paused polymerases at other repressed promoters in yeast such as *CYC1* and have been unable to identify any examples (Martens et al., 2001). In combination with my data, these observations suggest that yeast may not use deliberately stalled polymerase as a gene regulatory mechanism.

Materials and Methods:

Yeast strain construction and media

All strains used in this study are listed in Table 2.1 and were derived from W303-1a. All plasmids are listed in Table 2.2 and oligonucleotides are listed in Table 2.3. Standard mating and sporulation techniques were used to perform yeast crosses and isolate tetrads. The *T7pro::a1* allele, consisting of a 20bp minimal, optimal T7 promoter fused to the wild-type *a1* ORF including 5bp directly upstream of the ATG, to allow for T7 polymerase initiation, was synthesized on a plasmid (Mr. Gene GmbH, Germany) containing 50bp of homology matching the native *HMR a1* locus upstream and downstream of the *T7pro::a1* allele (pJR3208). The *T7pro::a1* allele and homology regions were amplified by PCR and transformed into JRY8676. Transformants were counter-selected with 5-FOA and -uracil medium. 5-FOA^r colonies were further screened by colony PCR. The resulting putative transformants were verified by sequencing. All further strains bearing *HMR T7pro::a1* were generated by standard mating and tetrad dissection, and segregates were verified by colony

PCR and sequencing to confirm the presence of the *T7pro::a1* allele in individual spores. Strains bearing *GAL1pro::a1* alleles were constructed in an identical fashion from a synthesized plasmid containing 450bp of the *GAL1* promoter directly upstream of *HMRa1* (pJR3209) (Mr. Gene GmbH, Germany).

The *gal4L331P* allele was provided by the Johnston lab on a plasmid and cloned into the HYG plasmid backbone of pJR2781 using BamHI and HindI digestion and ligation. The resulting plasmid was pJR3210. Wild-type *GAL4* was also cloned into pJR 2781 from genomic DNA using an identical protocol resulting in pJR3211. Both plasmids were verified by sequencing and then transformed into *gal4*Δ yeast strains for analysis.

For galactose induction experiments cells were grown to OD600 ≈ .7 in CSM raffinose or CSM-Leu raffinose (2%); then pre-warmed 20% galactose was added to a final concentration of 2%. All solution percentages are wt/vol. Fresh CSM galactose or CSM-Leu galactose media was added to kinetic experiments to maintain culture volume and OD over time. All medias in non-kinetic experiments were 2% sugar final concentration.

Potassium permanganate transcription bubble assay

10 OD units of exponentially growing cells (OD_{600}≈.9-1) grown in CSM or CSM-5mM nicotinamide were spun down and resuspended in 1ml cold PBS. These whole cells or 12µg genomic DNA was reacted with 20mM $KMnO_4$ on ice for times depicted in Figure 2.1. The reaction was halted using an excess of a 20mM ED Tris-Cl, 20mM EDTA, 1% SDS, .4M β-ME stop solution. DNA was extracted from whole cells using glass bead lysis and phenol-chloroform extraction and then precipitated using sodium-acetate and ethanol. Both genomic DNA reacted with $KMnO_4$ and DNA extracted from $KMnO_4$ treated whole cells was then resuspended in TE and stored at 4°C. A G/A genomic DNA ladder was generated by three-minute reaction of 5 µg yeast genomic DNA with 95% formic acid. The G/A ladder reaction was stopped and DNA was recovered using ethanol precipitation. Modified bases in the naked DNA and live cell DNA samples were converted to double strand breaks using piperidine as described in (Gilmour and Fan, 2009). LM-PCR analysis was performed as described in (Gilmour and Fan, 2009) using HPLC-PAGE purified linker primers and *HML**α**1* specific LM-PCR primers to amplify and label *HML**α***1 LM-PCR products. Radioactive LM-PCR products were resolved on a 40cm 19:1 Acrylamide:Bis-Acrylamide 6% urea sequencing gel, which was then dried on Whatman paper. Radioactivity patterns in the gel were recovered and visualized by exposure in a phosphor-imager cassette for 5 days and subsequently scanned in a phosphor-imager cassette on a Typhoon scanner (GE Healthcare) set to read storage phosphor screens.

mRNA extraction, cDNA preparation and analysis

Cultures were gown to an OD_{600}≈.75 and RNA was purified using the Qiagen RNAeasy kit (Qiagen) and on-column DNAse digestion (Qiagen). cDNA was prepared from 2µg total RNA using random hexamer or oligo dT primers as described and the Superscript III cDNA synthesis kit (Invitrogen). cDNA was then quantified by qPCR using the Dynamo SYBR green qPCR kit (NEB) and detected on a Stratagene MX3000 quantitative PCR system. All primer sets were normalized to *ACT1* amplification levels. Samples were analyzed in technical triplicate for at least 3 independent RNA preparations.

Whole cell extract preparation and immunoblotting

Cells were grown to an OD_{600}≈.75 and protein was extracted using 20% trichloroacetic acid and soluabilized in SDS sample buffer. Whole cell extracts were run on standard 10% SDS-PAGE gels and transferred to nitrocellulose membranes by wet-transfer at 150V for 1 hour. Immunoblotting followed standard protocols and blots were imaged on a LiCOR odyssey imager using secondary antibodies conjugated to IR dyes. Antibodies used in immunoblots were anti-T7 polymerase (Millipore 70566) and anti-Pgk1 (Invitrogen 459250).

Patch mating and sporulation assay

Diploid strains for the sporulation assay in Figure 2.2c were generated by mating JRY9520 with either JRY4012 or JRY8847 on YPD medium and selecting for diploids by replica plating onto media lacking uracil with 200 µg/ml hygromycin B. Sporulation in diploids was then assayed visually using a light microscope and a hemocytometer daily to quantify the percentage of cells that had sporulated in Spo media with galactose and 10mM nicotinamide.

Patch mating assays shown in Figure 2.6c were performed by mixing query strains on a plate with mating type tester strains prototrophic for all markers except *his4* (JRY2726, *MAT**a*** or JRY2728 *MAT**α***) on rich medium containing either 2% dextrose or 2% galactose and replica plating to minimal media plates with either 2% dextrose or 2% galactose.

Chromatin immuno-precipitation assay

All cells were cross-linked with 1% formaldehyde at OD_{600}≈.6-.9 for 20 minutes at room temperature and then quenched with glycine to a final concentration of 300mM for 5 min at room temperature. Cells were washed twice with cold Tris-buffered saline and lysed with .5mm zirconia beads in FA-lysis buffer (Aparicio et al., 2005) with protease inhibitors (Roche) in a MP Fastprep-24. Chromatin was isolated as described (Aparicio et al., 2005). For 13XMYC-Sir3 immunoprecipitations, 50µl of anti-myc agarose beads (Sigma E6654) were incubated overnight at 4°C with sonicated chromatin from 42.5mls of culture. For Gal4 immunoprecipitations, 4ul of anti-Gal4 antibody (Abcam 1396) and 25ul protein A sepharose (GE healthcare) was incubated overnight at

4°C with sonicated chromatin from 42.5mls of culture. Resin washes, elution, and DNA purification was performed as described (Aparicio et al., 2005). Precipitated DNA fragments were analyzed by qPCR as described previously. The negative control primer set for 13XMYC-Sir3 ChIP, *ARS504,* was chosen because it gave a consistently low IP/Input signal indistinguishable from a no-tag control and has not been shown to be bound by Sir3. Gal4 ChIP was normalized to a region downstream of the GAL1 gene not bound by Gal4. ChIP values are presented as enrichment relative to a control locus $((IP_{(primer)}/IN_{(primer)})/(IP_{(control)}/IN_{(control)}))$.

ChIP-Seq sample preparation and analysis

350 OD units (A600) of logarithmically growing cells were cross-linked with 1% formaldehyde for 15min at room temperature. Nuclei were prepared as in (Furuyama and Biggins, 2007) with the following modifications. Cells were resuspended in 4 ml/g cell weight Buffer 1 and digested with 450 ug Zymolyase-100T. Spheroplasts were washed twice in 5 mls SPC + Protease Inhibitors and resuspended in 1 ml SPC + PI. This resuspension was added to 1 ml Ficoll buffer while gently stirring. Nuclei were collected by spinning at 9800 rcf for 20 min at 4°C. Nuclei were washed twice with 1 ml SPC + protease inhibitors. Nuclei were resuspended in a final volume of 1 ml SPC + protease inhibitors and flash frozen at -80°C overnight. 420 units of MNase (Worthington) was added to thawed nuclei and nuclei were digested for 20 min at 37°C. Cells were pelleted at 3700 rpm for 10 min at 4°C. Supernatant was passed four times through a 20 gauge needle and then four times through 25 gauge needle and spun twice at 1300 rcf at 4°C. This clarified MNase digested chromatin was used for immunoprecipitations.

Libraries were constructed using the Illumina Tru-Seq library preparation kit with the following modifications. Upon end repair samples were cleaned up using a Qiagen minelute column. Adapters were used at a 10-fold diluted concentration as to that provided. Samples were indexed and sequenced in a single lane on the Illumina HiSeq 2000 as 100 bp paired-end reads.

Reads were mapped using BWA (Li and Durbin, 2009) to a modified Sac Cer 2 genome in which the *MAT* locus was replaced with the Hyg-MX cassette and the a1 promoter was replaced with the T7 promoter. Mapped reads were then trimmed to 40 bp and only reads with an insert length less than 250 bp were used to ensure mononucleosome resolution. The reads were further processed, including coverage calculations, signal smoothing and peak detection using nucleR (Flores and Orozco, 2011). A threshold value of 50% was used for peak detection and peaks were filtered for those with a score greater than .4. Figure 2.5 was created using R (R Core team 2012). Median coverage was calculated for 100 bp windows, sliding along each chromosome in 50 bp steps. The genome-wide median was calculated by determining the median of the sliding windows for each data set.

Table 2.1: Yeast strains

Strain	Parent	Genotype	Source
JRY4012	W303	*MATa his3-11 leu2-3, 112 lys2 trp1-1 ura3-1 can1-100*	R. Rothstein
JRY4579	W303	*MATa sir4Δ::TRP1 his3-11 leu2-3, 112 lys2 trp1-1 ura3-1 can1-100*	P. Errada (Rine lab)
JRY8676	W303	*MATα HMRa1ORF::K.lactis URA3ORF sir4Δ::HIS3 ade2 his3 leu2 trp1 ura3*	O. Zill (Rine lab)
JRY9514	W303	*MATα HMR:T7pro::a1 ade2 his3 leu2 ura3 [pJR3207]*	This study
ResubmJRY9515	W303	*MATα HMR:T7pro::a1 sir4Δ::HIS3 ade2 his3 leu2 ura3 [pJR3207]*	This study
JRY9516	W303	*MATα ade2 his3 leu2 ura3 [pJR3207]*	This study
JRY9517	W303	*MATα sir4Δ::HIS3 ade2 his3 leu2 ura3 [pJR3207]*	This study
JRY9518	W303	*MATα HMR:T7pro::a1 sir4Δ::HIS3 ade2 his3 leu2 ura3 [pJR1237]*	This study
JRY9519	W303	*MATα HMR:a2/a1promoterΔ sir4Δ::HIS3 ade2 his3 leu2 trp1 ura3*	This study
JRY9520	W303	*MATα HMR:T7pro::a1 sir4Δ::HIS3 URA3:GAL1promoterNLS-T7polymerase ade2 his3 leu2 ura3*	This study
JRY9521	W303	*MATα HMR:T7pro::a1 sir4Δ::HIS3 URA3:GAL1promoterNLS-T7polymerase ade2 his3 leu2 ura3 / MATa his3-11 leu2-3, 112 lys2 trp1-1 ura3-1 can1-100*	This study
JRY9522	W303	*MATα HMR:T7pro::a1 sir4Δ::HIS3 URA3:GAL1promoterNLS-T7polymerase ade2 his3 leu2 ura3 / matΔ::KANMX hmrΔ::HYGMX hmlΔ::NATMX ade2 his3 leu2 trp1 ura3*	This study
JRY9523	W303	*MATα HMR:T7pro::a1 13xMYC-SIR3:KANMX ade2 his3 leu2 trp1 ura3 [pJR3207]*	This study
JRY9524	W303	*MATα HMR:T7pro::a1 13xMYC-SIR3:KANMX sir4Δ::HIS3 ade2 his3 leu2 trp1 ura3 [pJR3207]*	This study
JRY9525	W303	*matΔ::HYGMX HMR:T7pro::a1 13xMYC-SIR3::KANMX ade2 his3 leu2 trp1 ura3*	This study
JRY9526	W303	*MATα HMR:GAL1pro::a1 13xMYC-SIR3:KANMX ade2 his3 leu2 trp1 ura3*	This study
JRY9527	W303	*MATα HMR:GAL1pro::a1 13xMYC-SIR3:KANMX sir4Δ::HIS3 ade2 his3 leu2*	This study

		trp1 ura3	
JRY4013	W303	*MATα his3-11 leu2-3, 112 lys2 trp1-1 ura3-1 can1-100*	R. Rothstein
JRY2726	W303	*MATa his4*	D. Botstein
JRY2728	W303	*MATα his4*	D. Botstein
JRY9528	W303	*MATα HMR:GAL1pro::a1 13xMYC-SIR3:KANMX gal4Δ::NATMX ade2 his3 leu2 trp1 ura3 [pJR3210]*	This study
JRY9529	W303	*MATα HMR:GAL1pro::a1 13xMYC-SIR3:KANMX gal4Δ::NATMX ade2 his3 leu2 trp1 ura3 [pJR3211]*	This study
JRY9530	W303	*MATα HMR:GAL1pro::a1 13xMYC-SIR3:KANMX sir4Δ::HIS3 gal4Δ::NATMX ade2 his3 leu2 trp1 ura3 [pJR3210]*	This study
JRY9531	W303	*MATα HMR:GAL1pro::a1 13xMYC-SIR3:KANMX sir4Δ::HIS3 gal4Δ::NATMX ade2 his3 leu2 trp1 ura3 [pJR3211]*	This study

Table 2.2: Yeast and bacterial plasmids

Plasmid	Backbone	Bacteria selection	Yeast selection	Insert	Source
pJR3207	pUC18	Amp	*LEU2*	GAL1pro:NLS-T7 Polymerase	Benton et al., 1990
pJR1237	pRS425	Amp	*LEU2*	empty vector	Brachmann et al. 1998
pJR3208	pMA-T	Amp	none	*T7pro::a1* cloning homology	This study, Mr. Gene
pJR3209	pMK-RQ	Kan	none	*GAL1pro::a1* cloning homology	This study, Mr. Gene
pJR2781	pRS41H	Amp	*HYG*	empty vector	Taxis and Knop 2006
pJR3210	pRS41H	Amp	*HYG*	*gal4L331P*	This study
pJR3211	pRS41H	Amp	*HYG*	*GAL4*	This study

Table 2.3: Oligonucleotides

Name	**Sequence**
LM-PCR	
LMPCR linker A (HPLC/PAGE Purified)	GCGGTGATTTAAAAGATCTGAATTC

LMPCR Linker B (HPLC/PAGE Purified)	GAATTCAGATC
HMLα1-LM-PCR-1	TGCTCAGCTAGACGTTTTTC
HMLα1-LM-PCR-2	CGTTTTTCTTTCAGCTTTTTTGA
HMLα1-LM-PCR-3	CAGCTTTTTTGAAACCGCTGTG
Strain construction	
T7pro::a1/GAL1pro::a1 knock in primer at *HMR* F	TTTTTCTGTGTAAGTTGATAATTACTTCTATCGTTTTCTATGCTGCGCAT
T7pro::a1/GAL1pro::a1 knock in primer at *HMR* R	GAAACTAAAAGAAAAACCCGACTATGCTATTTTAATCATTGAAAACGAAT
GAL4 KO F	ATCATTTTAAGAGAGGACAGAGAAGCAAGCCTCCTGAAAGCGGATCCCCGGGTTAATTAA
GAL4 KO R	GAAGTGAACTTGCGGGGTTTTTCAGTATCTACGATTCATTCGATGAATTCGAGCTCGTTT
qPCR	
a1 qPCRr F	TGGATGATATTTGTAGTATGGCGGA
a1 qPCR R	TCCCTTTGGGCTCTTCTCTT
ACT1 qPCR F	TGTCCTTGTACTCTTCCGGT
ACT1 qPCR R	CCGGCCAAATCGATTCTCAA
ARS504 qPCR F	GTCAGACCTGTTCCTTTAAGAGG
ARS504 qPCR R	CATACCCTCGGGTCAAACAC
TEL VIR 1.2kb qPCR F	GTGCTAAAGGAATCCCCAGAGA
TEL VIR 1.2kb qPCR R	TCTGTCCATTTTCCCTCTGCTC
HMR E qPCR F	CGAACGATCCCCGTCCAAGTTATGAGC
HMR E qPCR R	CAGGAGTACCTGCGCTTATTCTCAAAC
HMR I qPCR F	AGTTTCAGCTTTCCGCAACAGT
HMRa1 3' qPCR F	CCAACATTTTCGTATATGGCG
HMRa1 3' qPCR R	CTTGTGCAAATTCCAACTAAAGG
HMR a2 C qPCR F	CTTCTATCGTTTTCTATGCTGCG
GAL1 promoter qPCR F	GAGCCCCATTATCTTAGCCTAAAAAAAC
GAL1 promoter qPCR R	TACTGCCAATTTTTCCTCTTCATAACC

GAL1 3' ORF qPCR F	GAACGAGTCTCAAGCTTCTTGC
GAL1 3' ORF qPCR R	GCTGGTTTAGAGACGATGATAGC

References

Aparicio, O., Geisberg, J.V., Sekinger, E., Yang, A., Moqtaderi, Z., and Struhl, K. (2005). Chromatin Immunoprecipitation for Determining the Association of Proteins with Specific Genomic Sequences In Vivo. Curr Protoc Mol Biol *Chapter 21*, Unit21.3.

Armache, K.J., Garlick, J.D., Canzio, D., Narlikar, G.J., and Kingston, R.E. (2011). Structural Basis of Silencing: Sir3 BAH Domain in Complex with a Nucleosome at 3.0 Å Resolution. Science *334*, 977–982.

Beinoravičiūtė-Kellner, R., Lipps, G., and Krauss, G. (2005). In vitro selection of DNA binding sites for ABF1 protein from *Saccharomyces cerevisiae*. FEBS Lett. *579*, 4535–4540.

Benton, B.M., Eng, W.K., Dunn, J.J., Studier, F.W., Sternglanz, R., and Fisher, P.A. (1990). Signal-mediated import of bacteriophage T7 RNA polymerase into the Saccharomyces cerevisiae nucleus and specific transcription of target genes. Molecular and Cellular Biology *10*, 353–360.

Bernstein, B.E., Humphrey, E.L., Erlich, R.L., Schneider, R., Bouman, P., Liu, J.S., Kouzarides, T., and Schreiber, S.L. (2002). Methylation of histone H3 Lys 4 in coding regions of active genes. Proc. Natl. Acad. Sci. U.S.a. *99*, 8695–8700.

Borggrefe, T., Davis, R., Bareket-Samish, A., and Kornberg, R.D. (2001). Quantitation of the RNA Polymerase II Transcription Machinery in Yeast. J. Biol. Chem. *276*, 47150–47153.

Bunker, C.A., and Kingston, R.E. (1996). Activation domain-mediated enhancement of activator binding to chromatin in mammalian cells. Proc. Natl. Acad. Sci. U.S.a. *93*, 10820–10825.

Canzio, D., Chang, E.Y., Shankar, S., Kuchenbecker, K.M., Simon, M.D., Madhani, H.D., Narlikar, G.J., and Al-Sady, B. (2011). Chromodomain-Mediated Oligomerization of HP1 Suggests a Nucleosome-Bridging Mechanism for Heterochromatin Assembly. Molecular Cell *41*, 67–81.

Chen, L., and Widom, J. (2005). Mechanism of Transcriptional Silencing in Yeast. Cell *120*, 37–48.

Churchman, L.S., and Weissman, J.S. (2012). Nascent transcript sequencing visualizes transcription at nucleotide resolution. Nature *469*, 368–373.

Cosma, M.P. (2004). Daughter-specific repression of *Saccharomyces cerevisiae HO*: Ash1 is the commander. EMBO Rep. *5*, 953–957.

Deitsch, K.W., del Pinal, A., and Wellems, T.E. (1999). Intra-cluster recombination and *var* transcription switches in the antigenic variation of

Plasmodium falciparum. Mol. Biochem. Parasitol. *101*, 107–116.

Dellino, G.I., Schwartz, Y.B., Farkas, G., McCabe, D., Elgin, S.C.R., and Pirrotta, V. (2004). Polycomb Silencing Blocks Transcription Initiation. Molecular Cell *13*, 887–893.

Domergue, R., Castaño, I., Las Peñas, De, A., Zupancic, M., Lockatell, V., Hebel, J.R., Johnson, D., and Cormack, B.P. (2005). Nicotinic acid limitation regulates silencing of *Candida* adhesins during UTI. Science *308*, 866–870.

Dower, K., and Rosbash, M. (2002). T7 RNA polymerase-directed transcripts are processed in yeast and link 3' end formation to mRNA nuclear export. Rna *8*, 686–697.

Ehrentraut, S., Hassler, M., Oppikofer, M., Kueng, S., Weber, J.M., Mueller, J.W., Gasser, S.M., Ladurner, A.G., and Ehrenhofer-Murray, A.E. (2011). Structural basis for the role of the Sir3 AAA+ domain in silencing: interaction with Sir4 and unmethylated histone H3K79. Genes & Development *25*, 1835–1846.

Fascher, K.D., Schmitz, J., and Hörz, W. (1993). Structural and Functional Requirements for the Chromatin Transition at the *PHO5* Promoter in *Saccharomyces cerevisiae* upon *PHO5* Activation. J. Mol. Biol. *231*, 658–667.

Fitzgerald, D.P., and Bender, W. (2001). Polycomb Group Repression Reduces DNA Accessibility. Molecular and Cellular Biology *21*, 6585–6597.

Flanagan, P.M., Kelleher, R.J., Feaver, W.J., Lue, N.F., LaPointe, J.W., and Kornberg, R.D. (1990). Resolution of factors required for the initiation of transcription by yeast RNA polymerase II. J. Biol. Chem. *265*, 11105–11107.

Flores, O., and Orozco, M. (2011). nucleR: a package for non-parametric nucleosome positioning. Bioinformatics *27*, 2149–2150.

Fox, C.A., Ehrenhofer-Murray, A.E., Loo, S., and Rine, J. (1997). The Origin Recognition Complex, *SIR1*, and the S Phase Requirement for Silencing. Science *276*, 1547–1551.

Furuyama, S., and Biggins, S. (2007). Centromere identity is specified by a single centromeric nucleosome in budding yeast. Proc. Natl. Acad. Sci. U.S.a. *104*, 14706–14711.

Gao, L., and Gross, D.S. (2008). Sir2 Silences Gene Transcription by Targeting the Transition between RNA Polymerase II Initiation and Elongation. Molecular and Cellular Biology *28*, 3979–3994.

Gartenberg, M.R., Neumann, F.R., Laroche, T., Blaszczyk, M., and Gasser, S.M. (2004). Sir-Mediated Repression Can Occur Independently of Chromosomal and Subnuclear Contexts. Cell *119*, 955–967.

Gasser, S.M., Hediger, F., Taddei, A., Neumann, F.R., and Gartenberg, M.R. (2004). The Function of Telomere Clustering in Yeast: The Circe Effect. Cold Spring Harbor Symposia on Quantitative Biology *69*, 327–338.

Giardina, C., Perez-Riba, M., and Lis, J.T. (1992). Promoter melting and TFIID complexes on Drosophila genes in vivo. Genes & Development *6*, 2190–2200.

Giardina, C., and Lis, J.T. (1993). DNA melting on yeast RNA polymerase II promoters. Science *261*, 759–762.

Gilmour, D.S., and Fan, R. (2009). Detecting transcriptionally engaged RNA polymerase in eukaryotic cells with permanganate genomic footprinting. Methods *48*, 368–374.

Giniger, E., and Ptashne, M. (1988). Cooperative DNA binding of the yeast transcriptional activator GAL4

Gottschling, D.E. (1992). Telomere-proximal DNA in *Saccharomyces cerevisiae* is refractory to methyltransferase activity *in vivo*. Proc. Natl. Acad. Sci. U.S.a. *89*, 4062–4065.

Gottschling, D.E., Aparicio, O.M., Billington, B.L., and Zakian, V.A. (1990). Position effect at *S. cerevisiae* telomeres: reversible repression of Pol II transcription. Cell *63*, 751–762.

Haber, J.E., and George, J.P. (1979). A mutation that permits the expression of normally silent copies of mating-type information in *Saccharomyces cerevisiae* . Genetics *93,* 13-35.

Haber, J.E. (1998). Mating-type gene switching in *Saccharomyces cerevisiae*. Annu. Rev. Genet. *32*, 561–599.

Heard, E., Rougeulle, C., Arnaud, D., Avner, P., Allis, C.D., and Spector, D.L. (2001). Methylation of Histone H3 at Lys-9 Is an Early Mark on the X chromosome during X Inactivation. Cell *107*, 727–738.

Hecht, A., Strahl-Bolsinger, S., and Grunstein, M. (1996). Spreading of transcriptional repressor *SIR3* from telomeric heterochromatin. Nature *383*, 92–96.

Hengartner, C.J., Myer, V.E., Liao, S.M., Wilson, C.J., Koh, S.S., and Young, R.A. (1998). Temporal Regulation of RNA Polymerase II by Srb10 and Kin28 Cyclin-Dependent Kinases. Molecular Cell *2*, 43–53.

Herskowitz, I. (1988). Life cycle of the budding yeast *Saccharomyces cerevisiae*. Microbiol. Rev. *52*, 536–553.

Hickman, M.A., Froyd, C.A., and Rusche, L.N. (2011). Reinventing

Heterochromatin in Budding Yeasts: Sir2 and the Origin Recognition Complex Take Center Stage. Eukaryotic Cell *10*, 1183–1192.

Hoppe, G.J., Tanny, J.C., Rudner, A.D., Gerber, S.A., Danaie, S., Gygi, S.P., and Moazed, D. (2002). Steps in Assembly of Silent Chromatin in Yeast: Sir3-Independent Binding of a Sir2/Sir4 Complex to Silencers and Role for Sir2-Dependent Deacetylation. Molecular and Cellular Biology *22*, 4167–4180.

Huang, J., and Moazed, D. (2003). Association of the RENT complex with nontranscribed and coding regions of rDNA and a regional requirement for the replication fork block protein Fob1 in rDNA silencing. Genes & Development *17*, 2162–2176.

Imai, S., Armstrong, C.M., Kaeberlein, M., and Guarente, L. (2000). Transcriptional silencing and longevity protein Sir2 is an NAD-dependent histone deacetylase. Nature *403*, 795–800.

Johnson, A., Li, G., Sikorski, T.W., Buratowski, S., Woodcock, C.L., and Moazed, D. (2009). Reconstitution of Heterochromatin-Dependent Transcriptional Gene Silencing. Molecular Cell *35*, 769–781.

Johnson, A., Wu, R., Peetz, M., Gygi, S.P., and Moazed, D. (2013). Heterochromatic gene silencing by activator interference and a transcription elongation barrier. J. Biol. Chem. *288*, 28771–28782.

Johnston, M., and Dover, J. (1988). Mutational analysis of the GAL4-encoded transcriptional activator protein of Saccharomyces cerevisiae. Genetics *120*, 63–74.

Kayne, P.S., Kim, U.J., Han, M., Mullen, J.R., Yoshizaki, F., and Grunstein, M. (1988). Extremely Conserved Histone H4 N Terminus Is Dispensable for Growth but Essential for Repressing the Silent Mating Loci in Yeast. Cell *55*, 27–39.

Kitada, T., Kuryan, B.G., Tran, N.N.H., Song, C., Xue, Y., Carey, M., and Grunstein, M. (2012). Mechanism for epigenetic variegation of gene expression at yeast telomeric heterochromatin. Genes & Development *26*, 2443–2455.

Klar, A.J., Fogel, S., and Macleod, K. (1979). *MAR1*--A regulator of the *HMa* and *HMalpha* loci in *Saccharomyces cerevisiae*. Genetics *93,* 37-50.

Komachi, K., Redd, M.J., and Johnson, A.D. (1994). The WD repeats of Tup1 interact with the homeo domain protein alpha 2. Genes & Development *8*, 2857–2867.

Kornberg, R.D. (2007). The molecular basis of eukaryotic transcription. Proc. Natl. Acad. Sci. U.S.a. *104*, 12955–12961.

Landry, J., Sutton, A., Tafrov, S.T., Heller, R.C., Stebbins, J., Pillus, L., and

Sternglanz, R. (2000). The silencing protein SIR2 and its homologs are NAD-dependent protein deacetylases. Proc. Natl. Acad. Sci. U.S.a. *97*, 5807–5811.

la Paz Sanchez, de, M., and Gutierrez, C. (2009). Arabidopsis ORC1 is a PHD-containing H3K4me3 effector that regulates transcription. Proceedings of the National Academy of Sciences *106*, 2065–2070.

Lee, T.I., and Young, R.A. (2000). Transcription of eukaryotic protein-coding genes. Annu. Rev. Genet. *34*, 77–137.

Li, H., and Durbin, R. (2009). Fast and accurate short read alignment with Burrows-Wheeler transform. Bioinformatics *25*, 1754–1760.

Li, J., Coïc, E., Lee, K., Lee, C.-S., Kim, J.-A., Wu, Q., and Haber, J.E. (2012). Regulation of Budding Yeast Mating-Type Switching Donor Preference by the FHA Domain of Fkh1. PLoS Genet *8*, e1002630.

Loo, S., and Rine, J. (1994). Silencers and Domains of Generalized Repression. Science *264*, 1768–1771.

Lorch, Y., LaPointe, J.W., and Kornberg, R.D. (1992). Initiation on chromatin templates in a yeast RNA polymerase II transcription system. Genes & Development *6*, 2282–2287.

Lynch, P.J., and Rusche, L.N. (2008). A Silencer Promotes the Assembly of Silenced Chromatin Independently of Recruitment. Molecular and Cellular Biology *29*, 43–56.

Mai, X., Chou, S., and Struhl, K. (2000). Preferential Accessibility of the Yeast *his3* Promoter Is Determined by a General Property of the DNA Sequence, Not by Specific Elements. Molecular and Cellular Biology *20*, 6668–6676.

Martens, C., Krett, B., and Laybourn, P.J. (2001). RNA polymerase II and TBP occupy the repressed *CYC1* promoter. Mol. Microbiol. *40*, 1009–1019.

McBroom, L.D., and Sadowski, P.D. (1995). Functional analysis of the ABF1-binding sites within the Ya regions of the *MATa* and *HMRa* loci of *Saccharomyces cerevisiae*. Current Genetics *28*, 1–11.

McCall, K., and Bender, W. (1996). Probes of chromatin accessibility in the *Drosophila* bithorax complex respond differently to *Polycomb*-mediated repression. The EMBO Journal *15*, 569–580.

Miele, A., Bystricky, K., and Dekker, J. (2009). Yeast Silent Mating Type Loci Form Heterochromatic Clusters through Silencer Protein-Dependent Long-Range Interactions. PLoS Genet *5*, e1000478.

Mishra, K., and Shore, D. (1999). Yeast Ku protein plays a direct role in telomeric

silencing and counteracts inhibition by rif proteins. Curr. Biol. *9*, 1123–1126.

Moazed, D., Kistler, A., Axelrod, A., Rine, J., and Johnson, A.D. (1997). Silent information regulator protein complexes in *Saccharomyces cerevisiae*: a SIR2/SIR4 complex and evidence for a regulatory domain in SIR4 that inhibits its interaction with SIR3. Proc. Natl. Acad. Sci. U.S.a. *94*, 2186–2191.

Moretti, P., Freeman, K., Coodly, L., and Shore, D. (1994). Evidence that a complex of SIR proteins interacts with the silencer and telomere-binding protein RAP1. Genes & Development *8*, 2257–2269.

Musladin, S., and Barbarić, S. (2010). Yeast *PHO* genes: An excellent model for elucidation of chromatin-remodelling mechanisms. Food Technology and Biotechnology *48*, 308–316.

Mylin, L.M., Johnston, M., and Hopper, J.E. (1990). Phosphorylated forms of GAL4 are correlated with ability to activate transcription. Molecular and Cellular Biology *10*, 4623–4629.

Nagalakshmi, U., Wang, Z., Waern, K., Shou, C., Raha, D., Gerstein, M., and Snyder, M. (2008). The Transcriptional Landscape of the Yeast Genome Defined by RNA Sequencing. Science *320*, 1344–1349.

Nislow, C., Ray, E., and Pillus, L. (1997). SET1, a Yeast Member of the *Trithorax* Family, Functions in Transcriptional Silencing and Diverse Cellular Processes. Mol. Biol. Cell *8*, 2421–2436.

Olave, I., Reinberg, D., and Vales, L.D. (1998). The mammalian transcriptional repressor RBP (CBF1) targets TFIID and TFIIA to prevent activated transcription. Genes & Development *12*, 1621–1637.

Osborne, E.A., Dudoit, S., and Rine, J. (2009). The establishment of gene silencing at single-cell resolution. Nat Genet *41*, 800–806.

Padmanabhan, K., Robles, M.S., Westerling, T., and Weitz, C.J. (2012). Feedback Regulation of Transcriptional Termination by the Mammalian Circadian Clock PERIOD Complex. Science *337*, 599–602.

Park, E.C., and Szostak, J.W. (1990). Point mutations in the yeast histone H4 gene prevent silencing of the silent mating type locus HML. Molecular and Cellular Biology *10*, 4932–4934.

Park, J.-H., Cosgrove, M.S., Youngman, E., Wolberger, C., and Boeke, J.D. (2002). A core nucleosome surface crucial for transcriptional silencing. Nat Genet *32*, 273–279.

Park, P.U., Defossez, P.A., and Guarente, L. (1999). Effects of mutations in DNA repair genes on formation of ribosomal DNA circles and life span in

Saccharomyces cerevisiae. Molecular and Cellular Biology *19*, 3848–3856.

Parnell, E.J., and Stillman, D.J. (2011). Shields up: the Tup1-Cyc8 repressor complex blocks coactivator recruitment. Genes & Development *25*, 2429–2435.

Piekarska, I., Rytka, J., and Rempola, B. (2010). Regulation of sporulation in the yeast *Saccharomyces cerevisiae.* Acta Biochim. Pol. *57*, 241–250.

Pillus, L., and Rine, J. (1989). Epigenetic inheritance of transcriptional states in *S. cerevisiae*. Cell *59*, 637–647.

Pinkham, J.L., Dudley, A.M., and Mason, T.L. (1994). T7 RNA Polymerase-Dependent Expression of COXII in Yeast Mitochondria. Molecular and Cellular Biology *14*, 4643–4652.

Pruitt, K., Zinn, R.L., Ohm, J.E., McGarvey, K.M., Kang, S.-H.L., Watkins, D.N., Herman, J.G., and Baylin, S.B. (2006). Inhibition of SIRT1 reactivates silenced cancer genes without loss of promoter DNA hypermethylation. PLoS Genet *2*, e40.

Radonjic, M., Andrau, J.-C., Lijnzaad, P., Kemmeren, P., Kockelkorn, T.T.J.P., van Leenen, D., van Berkum, N.L., and Holstege, F.C.P. (2005). Genome-Wide Analyses Reveal RNA Polymerase II Located Upstream of Genes Poised for Rapid Response upon *S. cerevisiae* Stationary Phase Exit. Molecular Cell *18*, 171–183.

Ravindra, A., Weiss, K., and Simpson, R.T. (1999). High-Resolution Structural Analysis of Chromatin at Specific Loci: *Saccharomyces cerevisiae* Silent Mating Type Locus *HMLa*. Molecular and Cellular Biology *19*, 7944–7950.

Ren, J., Wang, C.L., and Sternglanz, R. (2010). Promoter Strength Influences the S Phase Requirement for Establishment of Silencing at the *Saccharomyces cerevisiae* Silent Mating Type Loci. Genetics *186*, 551–560.

Rhee, H.S., and Pugh, B.F. (2013). Genome-wide structure and organization of eukaryotic pre-initiation complexes. Nature *483*, 295–301.

Rine, J., Strathern, J.N., Hicks, J.B., and Herskowitz, I. (1979). A suppressor of mating-type locus mutations in *Saccharomyces cerevisiae*: evidence for and identification of cryptic mating-type loci. Genetics *93,* 877-901.

Rine, J., and Herskowitz, I. (1987). Four genes responsible for a position effect on expression from *HML* and *HMR* in *Saccharomyces cerevisiae*. Genetics *116*, 9–22.

Rubin, C.M., and Schmid, C.W. (1980). Pyrimidine-specific chemical reactions useful for DNA sequencing. Nucleic Acids Research *8*, 4613–4620.

Rusche, L.N., Kirchmaier, A.L., and Rine, J. (2002). Ordered Nucleation and Spreading of Silenced Chromatin in S*accharomyces cerevisiae*. Mol. Biol. Cell *13*, 2207–2222.

Rusche, L.N., Kirchmaier, A.L., and Rine, J. (2003). The Establishment, Inheritance, and Function of Silenced Chromatin in *Saccharomyces cerevisiae*. Annu. Rev. Biochem. *72*, 481–516.

Sekinger, E.A., and Gross, D.S. (2001). Silenced Chromatin is Permissive to Activator Binding and PIC Recruitment. Cell *105*, 403–414.

Shogren-Knaak, M., Ishii, H., Sun, J.-M., Pazin, M.J., Davie, J.R., and Peterson, C.L. (2006). Histone H4-K16 Acetylation Controls Chromatin Structure and Protein Interactions. Science *311*, 844–847.

Sinclair, D.A., and Guarente, L. (1997). Extrachromosomal rDNA Circles—A Cause of Aging in Yeast. Cell *91*, 1033–1042.

Smith, J.S., Brachmann, C.B., Pillus, L., and Boeke, J.D. (1998). Distribution of a Limited Sir2 Protein Pool Regulates the Strength of Yeast rDNA Silencing and Is Modulated by Sir4p. Genetics *149*, 1205–1219.

Steinmetz, E.J., Warren, C.L., Kuehner, J.N., Panbehi, B., Ansari, A.Z., and Brow, D.A. (2006). Genome-Wide Distribution of Yeast RNA Polymerase II and Its Control by Sen1 Helicase. Molecular Cell *24*, 735–746.

Straight, A.F., Shou, W., Dowd, G.J., Turck, C.W., Deshaies, R.J., Johnson, A.D., and Moazed, D. (1999). Net1, a Sir2-associated nucleolar protein required for rDNA silencing and nucleolar integrity. Cell *97*, 245–256.

Strathern, J., Hicks, J., and Herskowitz, I. (1981). Control of Cell Type in Yeast by the Mating Type Locus: the α1-α2 hypothesis. J. Mol. Biol. *147*, 357–372.

Strathern, J.N., Klar, A.J., Hicks, J.B., Abraham, J.A., Ivy, J.M., Nasmyth, K.A., and McGill, C. (1982). Homothallic Switching of Yeast Mating Type Cassettes Is Initiated by a Double-Stranded Cut in the *MAT* Locus. Cell *31*, 183–192.

Talbert, P.B., and Henikoff, S. (2006). Spreading of silent chromatin: inaction at a distance. Nat Rev Genet *7*, 793–803.

Tanaka, M. (1996). Modulation of promoter occupancy by cooperative DNA binding and activation-domain function is a major determinant of transcriptional regulation by activators *in vivo*. Proc. Natl. Acad. Sci. U.S.a. *93*, 4311–4315.

Taylor, I.C., Workman, J.L., Schuetz, T.J., and Kingston, R.E. (1991). Facilitated binding of GAL4 and heat shock factor to nucleosomal templates: differential function of DNA-binding domains. Genes & Development *5*, 1285–1298.

Teytelman, L., Eisen, M.B., and Rine, J. (2008). Silent but Not Static: Accelerated Base-Pair Substitution in Silenced Chromatin of Budding Yeasts. PLoS Genet *4*, e1000247.

Teytelman, L., Ozaydin, B., Zill, O., Lefrançois, P., Snyder, M., Rine, J., and Eisen, M.B. (2009). Impact of chromatin structures on DNA processing for genomic analyses. PLoS ONE *4*, e6700.

Triolo, T., and Sternglanz, R. (1996). Role of interactions between the origin recognition complex and SIR1 in transcriptional silencing. Nature *381*, 251–253.

Um, M., Li, C., and Manley, J.L. (1995). The transcriptional repressor even-skipped interacts directly with TATA-binding protein. Molecular and Cellular Biology *15*, 5007–5016.

Ujvári, A., and Martin, C.T. (1997). Identification of a minimal binding element within the T7 RNA polymerase promoter. J. Mol. Biol. *273*, 775–781.

Valenzuela, L., Dhillon, N., Dubey, R.N., Gartenberg, M.R., and Kamakaka, R.T. (2008). Long-Range Communication between the Silencers of *HMR*. Molecular and Cellular Biology *28*, 1924–1935.

van Dijk, E.L., Chen, C.L., d'Aubenton-Carafa, Y., Gourvennec, S., Kwapisz, M., Roche, V., Bertrand, C., Silvain, M., Legoix-Né, P., Loeillet, S., et al. (2012). XUTs are a class of Xrn1-sensitive antisense regulatory non-coding RNA in yeast. Nature *475*, 114–117.

Waterborg, J.H. (2000). Steady-state Levels of Histone Acetylation in *Saccharomyces cerevisiae*. Journal of Biological Chemistry *275*, 13007–13011.

Weiss, K., and Simpson, R.T. (1998). High-Resolution Structural Analysis of Chromatin at Specific Loci: *Saccharomyces cerevisiae* Silent Mating Type Locus *HMLalpha*. Molecular and Cellular Biology *18*, 5392–5403.

Whitehouse, I., Rando, O.J., Delrow, J., and Tsukiyama, T. (2007). Chromatin remodelling at promoters suppresses antisense transcription. Nature *450*, 1031–1035.

XU, E., Zawdzki, K., and Broach, J. (2006). Single-Cell Observations Reveal Intermediate Transcriptional Silencing States. Molecular Cell *23*, 219–229.

Zeitlinger, J., Stark, A., Kellis, M., Hong, J.-W., Nechaev, S., Adelman, K., Levine, M., and Young, R.A. (2007). RNA polymerase stalling at developmental control genes in the *Drosophila melanogaster* embryo. Nat Genet *39*, 1512–1516.

Zhang, Z., and Dietrich, F.S. (2005). Mapping of transcription start sites in *Saccharomyces cerevisiae* using 5' SAGE. Nucleic Acids Research *33*, 2838–

2851.

Zill, O.A., Scannell, D., Teytelman, L., and Rine, J. (2010). Co-Evolution of Transcriptional Silencing Proteins and the DNA Elements Specifying Their Assembly. PLoS Biol *8*, e1000550.

Appendix I: A novel genetic interaction between *SIR2* and the *ASF1, RTT109* histone acetylation and incorporation pathway

The work in this appendix was performed in conjunction with an undergraduate researcher, Justin Feng.

Introduction:

Synthetic genetic array (SGA) technology allows the characterization of the phenotypes of almost all possible non-essential double mutants in yeast in a high-throughput fashion. (Tong et al., 2001). SGA technology and its derivatives accelerated the pace of discovery of previously unappreciated genetic interactions and pathways (Tong et al., 2004; Schuldiner et al., 2005; Collins et al., 2007; Costanzo et al., 2010). The interpretation of synthetic-genetic-array data is based on the principle that the fitness, or growth rate, of any double mutant, in the absence of a genetic interaction, should be the product of the fitness of the two single mutants. Deviations from the expected multiplicative fitness suggest the occurrence of an interaction between the two genes, resulting in synthetic sickness/lethality (SSL), or genetic suppression. Both SSL and genetic suppression demonstrate that two genes are interacting to produce a phenotype that neither gene is responsible for on its own.

SGA experiments proceed by mating a query strain with a single mutation in a gene of interest to a panel of yeast-deletion-collection single-mutant strains to generate diploids. Diploids are then sporulated and the spores are selected by growth on media that allows the growth of only double-mutant haploids, traditionally of a single mating type. However, because of the requirement for mating and selection steps to create high-throughput panels of double-mutant strains, not every yeast gene has been assayed using synthetic-genetic arrays. For example, strains with defects in mating, or sporulation, may not be able to complete the SGA double-mutant selection protocol, and thus have not been assayed.

Strains lacking Sir proteins display mating defects because derepression of *HML**α*** and *HMRa* leads to a pseudo-diploid phenotype (Rine and Herskowitz, 1987). Because *sir*Δ haploid cells are non-maters they were not included in original SGA analyses. The Nyström lab specifically addressed this limitation and created a *sir2*Δ *MAT**α*** *hml*Δ *hmr*Δ strain that is competent for mating, and thus could be used in a traditional SGA pipeline (Liu et al., 2010). Their high-throughput *sir2*Δ SGA screen identifies 122 SSL interactions with *sir2*Δ. They chose to follow up on a genetic interaction between *SIR2* and *BNI1* that demonstrates the importance of Sir2 for retrograde transport of damaged or aggregated proteins into the mother cell along actin cables during cell division. They did not address the implications of the remaining 121 SSL interactions

identified in this screen, most of which had no previously known link to *BNI1* or *SIR2* function.

We performed a targeted screen of the 121 remaining proposed *sir2*Δ genetic interactions identified by the Nyström lab to test the reproducibility and importance of the novel genetic interactions involving Sir2.

Results:

Identification and verification of *sir2*Δ genetic interactions

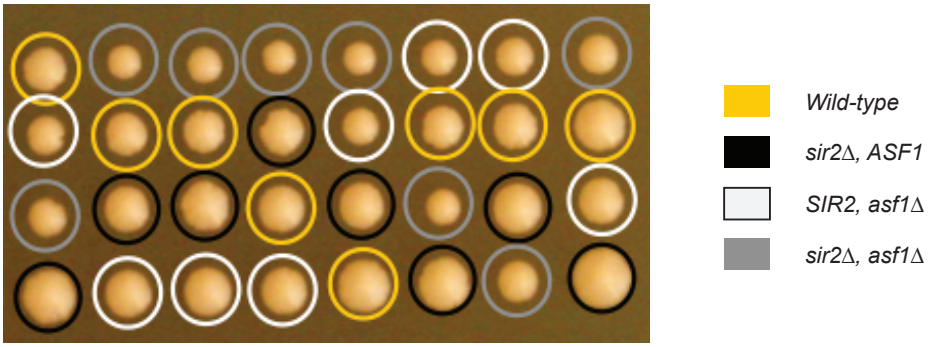
We sought to determine if *sir2*Δ SSL interactions identified via high-throughput screening could be replicated and verified by the most rigorous method of testing genetic interactions: tetrad analysis. To perform tetrad analysis, we requested the query strain used in the initial *sir2*Δ SGA analysis from the Nyström lab. The query strain was *MATα sir2*Δ *hml*Δ *hmr*Δ and contained the required markers for the SGA mating and selection protocol. We then mated the *sir2*Δ query strain to strains from the *MATa* deletion collection (Winzeler et al., 1999) corresponding to the interactions described in Liu et al., 2010 listed in Table AI.1 and selected for diploids. Diploids were sporulated and tetrads were dissected onto rich media.

To evaluate statistically the potential genetic interactions between *sir2*Δ and single-gene deletions we used quantitative image analysis. After 3-4 days of growth on rich media, plates containing the recently dissected spores were photographed, and the images were then imported to ImageJ analysis software (Abramoff et el., 2004). Then, because spores clones were grown on the same medium and for the same period of time before imagining, we measured colony size (pixels) as a proxy for growth rate. We replica plated the spores to selective media and assigned genotypes to each spore based on the results of replica plating. By comparing the number of pixels in each colony of known genotype, we were able to perform t-tests to determine if spores of different genotypes displayed statistically significant differences in growth. To label a SSL interaction between *sir2*Δ and a query gene (*yfg*Δ) as significant, we required a significant ($p<.05$) difference, as measured by a student's t-test, in the number of pixels of all colonies of *yfg*Δ single-mutants vs. all colonies of *sir2*Δ *yfg*Δ double mutants, and between the number of pixels of all colonies of *sir2*Δ single mutants vs. all colonies of *sir2*Δ *yfg*Δ double mutants. Query strains that did not satisfy both reciprocal t-test requirements for statistical significance were not labeled as having a SSL interaction (see Table AI.1). Representative tetrad plate images used in image analysis for *asf1*Δ and *rtt109*Δ are presented in Figure AI.1

Gene	*sir2*Δ
*asf1*Δ	synthetic sick
*rtt109*Δ	synthetic sick
*cac2*Δ	no significant interaction
*swr1*Δ	no significant interaction
*slx8*Δ	no significant interaction
*ctf4*Δ	no significant interaction
*elp4*Δ	no significant interaction
*hst1*Δ	no significant interaction
*hst3*Δ	no significant interaction
*mdm12*Δ	no significant interaction
*mek1*Δ	no significant interaction
*nup2*Δ	no significant interaction
*pho88*Δ	no significant interaction
*slx9*Δ	no significant interaction
*swc5*Δ	no significant interaction
*yjl055W*Δ	no significant interaction
*ama1*Δ	no significant interaction

Table AI.1: Results of *sir2*Δ-synthetic-genetic-interaction-tetrad analysis
A *MATα sir2*Δ query strain was mated to selected *MATa* yeast-deletion-collection strains to generate diploids, which were then sporulated. Tetrads were dissected onto rich media and genetic interactions were evaluated using a quantitative visual assay as described. Results are based on analysis of at least n=40 complete tetrads from two independent diploids.

SIR2 asf1Δ x sir2Δ ASF1



SIR2 rtt109Δ x sir2Δ RTT109

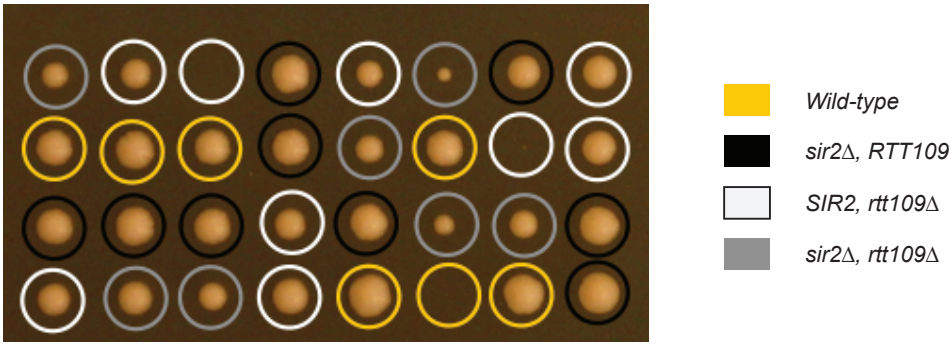


Figure AI.1: *sir2*Δ-synthetic-genetic-interaction-tetrad analysis images
A *MAT**α*** *sir2*Δ query strain was mated to *asf1*Δ or *rtt109*Δ *MATa* yeast-deletion-collection strains to generate diploids, which were then sporulated. Tetrads were dissected onto rich media and representative examples are shown here. Genetic interactions were evaluated using a quantitative visual assay as described. Results are based on analysis of at least n=40 complete tetrads from two independent diploids.

We were unable to replicate the majority of the SSL interactions reported in the genome-wide SGA analysis by the Nyström lab (Liu et al., 2010) in our focused, low-throughput assay. Of the 15 reported genetic interactions tested, we found only *asf1*Δ ($p<.005$) and *rtt109*Δ ($p<.005$) showed a repeatable, significant SSL interaction with *sir2*Δ. We also included two genes (*yjl055W*Δ, *ama1*Δ) not reported to interact with *sir2*Δ in our screen as a negative control for a lack of a *sir2*Δ SSL interaction. *yjl055W*Δ *and ama1*Δ behaved as expected. Asf1 is a histone chaperone involved in both transcription-coupled, and replication-coupled, chromatin assembly along with other factors such as the Hir-complex (Sharp et al., 2001). Rtt109 is a histone acetyl-transferase that acetylates H3-K56 on free histones to facilitate incorporation into chromatin (Driscoll et al., 2007; Han et al. 2007). Both Asf1 and Rtt109 operate together to assemble acetylated histones into chromatin, concurrent with transcription, or coupled with DNA replication (Tsubota et al., 2007; Kolonko et al., 2010).

To further challenge the apparent *sir2*Δ *asf1*Δ and *sir2*Δ *rtt109*Δ SSL interactions, we performed a kinetic growth-rate assay to measure growth rate of

wild-type, single-mutant, and double-mutant strains. We grew strains in rich media in microtiter plates and used a plate reader to periodically measure OD600, as a proxy for cell number, following each culture until it reached saturation. To compute growth rate, we measured the maximum slope of the OD600 curve during logarithmic growth (OD600 between 0.1 and 0.5). Using our kinetic growth assay we determined a growth rate for wild-type, single-mutant, and *sir2*Δ *asf1*Δ and *sir2*Δ *rtt109*Δ double-mutant spore progeny. The results of the growth-rate measurement are presented in Figure AI.2. In agreement with our tetrad analysis by visual assay, we showed that mutant alleles of *SIR2* and *RTT109* as well as mutant alleles of *SIR2* and *ASF1* showed SSL interactions as evidenced by the reduced growth rate of *sir2*Δ *asf1*Δ and *sir2*Δ *rtt109*Δ strains in comparison to wild-type, *sir2*Δ, *asf1*Δ, and *rtt109*Δ strains alone (Figure AI.2). We also observed a positive genetic interaction between *asf1*Δ and *rtt109*Δ: the growth rate of an *asf1*Δ *rtt109*Δ double-mutant strain was higher than expected based on the growth of *asf1*Δ or *rtt109*Δ strains alone.

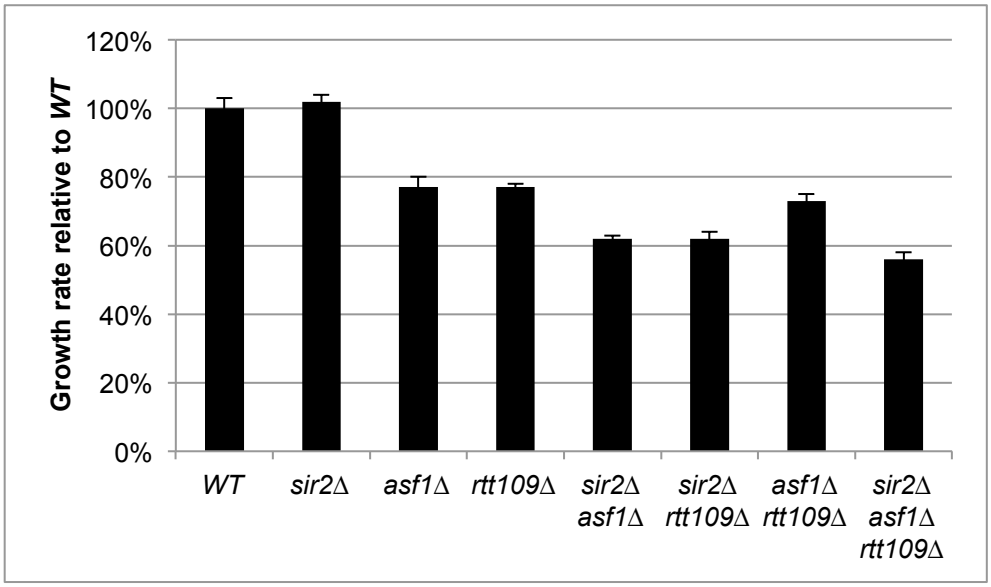


Figure AI.2: Growth rates of *sir2*Δ, *rtt109*Δ, and *asf1*Δ mutants in rich media liquid culture
Logarithmically-growing cells were seeded into 96-well plates in rich media at 30°C and OD600 was assayed every 30 minutes to monitor growth. Growth rates were calculated based on OD600 values as described in (Mayfield et al., 2012). Growth rate is presented relative to wild-type. Data are from at least n=3 independent spores. Error bars depict standard error. All strains assayed are isogenic and progeny of a single diploid parent.

To quantify the magnitude of the observed *sir2*Δ genetic interactions, we calculated ε-values. ε-values mathematically describe how far above or below the expected double-mutant fitness an actual double mutant falls, based on the observed fitness of each single mutant (Collins et al., 2006). Positive ε-values indicate genetic suppression and negative ε-values indicate synthetic sick interactions. It is impossible to calculate an ε-value for a synthetic lethal interaction because the non-existent double mutant has a fitness value of zero. Empirical evidence demonstrates that the maximum observed magnitude of a

negative ε-value is ≈.5 (Costanzo et al., 2010). To calculate ε, we used growth rate from our liquid culture assay as a proxy for fitness, and normalized growth rate of double and single mutants to the growth rate of wild-type. ε-values are calculated as ε = fitness(*sir2*Δ *yfg*Δ)-fitness(*sir2*Δ)•fitness(*yfg*Δ). The results of our ε-value calculations, presented in Table AI.2, demonstrated the large magnitude of SLL and genetic suppression interactions among the *sir2*Δ, *asf1*Δ, and *rtt109*Δ mutations. It was not possible to determine the statistical significance of our ε-values because we tested a small number of genetic interactions and did not have access to the complete empirical distribution of possible ε-values for simulations, but, when similar calculations were performed on genome-wide datasets, ε-values of similar magnitude were highly significant ($p<.001$) (Koh et al., 2010).

Genotype	Ε-value
*asf1*Δ *sir2*Δ	-0.1662
*rtt109*Δ *sir2*Δ	-0.1628
*asf1*Δ *rtt109*Δ	0.1299
*asf1*Δ *rtt109*Δ *sir2*Δ	-0.0437

Table AI.2: ε-values calculated based on kinetic growth rate
ε-values were calculated as ε = fitness(*sir2*Δ *yfg*Δ)-fitness(*sir2*Δ)•fitness(*yfg*Δ) from (Collins et al., 2006) based on kinetic growth-rate data presented in Figure AI.2.

SSL interactions between *sir2*Δ and *rtt109*Δ, *sir2*Δ and *asf1*Δ depend on the catalytic activity of Sir2

Having verified and quantitated the interactions among *sir2*Δ, *asf1*Δ, and *rtt109*Δ we then asked if the SSL interactions were dependent on the activity of Sir2 alone or reflected a defect in the Sir2/3/4-complex normally associated with transcriptional silencing. We performed tetrad analysis of *sir3*Δ and *sir4*Δ strains in combination with *asf1*Δ and *rtt109*Δ as described previously. We found no significant interaction between *sir3*Δ or *sir4*Δ and *asf1*Δ or *rtt109*Δ (Table AI.3). Thus, the interaction between *sir2*Δ and *asf1*Δ and *sir2*Δ and *rtt109*Δ was specific to *sir2*Δ alone.

Gene	***sir2N345A* (catalytically inactive)**	***sir3*Δ**	***sir4*Δ**
***asf1*Δ**	synthetic sick	no significant interaction	no significant interaction
***rtt109*Δ**	synthetic sick	no significant interaction	no significant interaction

Table AI.3: *sir2*Δ-synthetic-genetic interactions assayed by tetrad analysis
*MATα sir3*Δ*, sir4*Δ*,* or *sir2N345A* query strains were mated to *asf1*Δ and *rtt109*Δ *MATa* yeast-deletion-collection strains to generate diploids, which were then sporulated. Tetrads were dissected onto rich media and genetic interactions were evaluated using a quantitative visual assay as described. Results are based on analysis of at least n=40 complete tetrads from two independent diploids.

Having determined the interaction between nucleosome acetylation and incorporation proteins Asf1 and Rtt109 and Sir2 was specific to Sir2 alone, and not the transcriptional silencing Sir2/3/4-complex, we asked if the SSL interaction was dependent on the catalytic activity of Sir2. A single point mutation, *sir2N345A*, eliminates catalytic activity of Sir2 (Armstrong et al., 2002). We performed tetrad analysis with a strain bearing the *sir2N345A* catalytically inactive allele in combination with *asf1*Δ and *rtt109*Δ. We saw a significant SSL interaction between *sir2N345A* and *asf1*Δ or *rtt109*Δ as in *sir2*Δ strains, indicating the *SIR2 ASF1* and *SIR2 RTT109* genetic interactions required the catalytic activity of Sir2 (Table AI.3). The catalytic activity requirement of Sir2 for the SSL interaction was further reinforced by the behavior of a panel of *sir2*Δ, *asf1*Δ, and *rtt109*Δ mutants grown in nicotinamide (NAM)-containing medium (Figure AI.3). Nicotinamide is a chemical inhibitor of Sir2, and thus strains grown in medium with NAM behave similarly to *sir2*Δ cells if Sir2 catalysis is required for the SSL interaction. Both *rtt109*Δ and *asf1*Δ strains grown in nicotinamide media had similar growth rates to *sir2*Δ *asf1*Δ or *sir2*Δ *rtt109*Δ strains grown in standard media. Because nicotinamide inhibits NAD-dependent-histone-deactylase catalysis, and strains inhibited with nicotinamide showed a growth-rate defect similar to that of *sir2*Δ strains, we further confirmed the genetic interaction between *SIR2* and *ASF1* and *SIR2* and *RTT109* requires the catalytic activity of Sir2 and may have some contribution by other NAD-dependent histone deactylases such as *HST1-4*.

In summary we verified a negative-synthetic-genetic interaction between *SIR2* and the *ASF1*/*RTT109* histone acetylation and assembly pathway that is independent of the Sir2/3/4-complex and depends on the catalytic activity of Sir2.

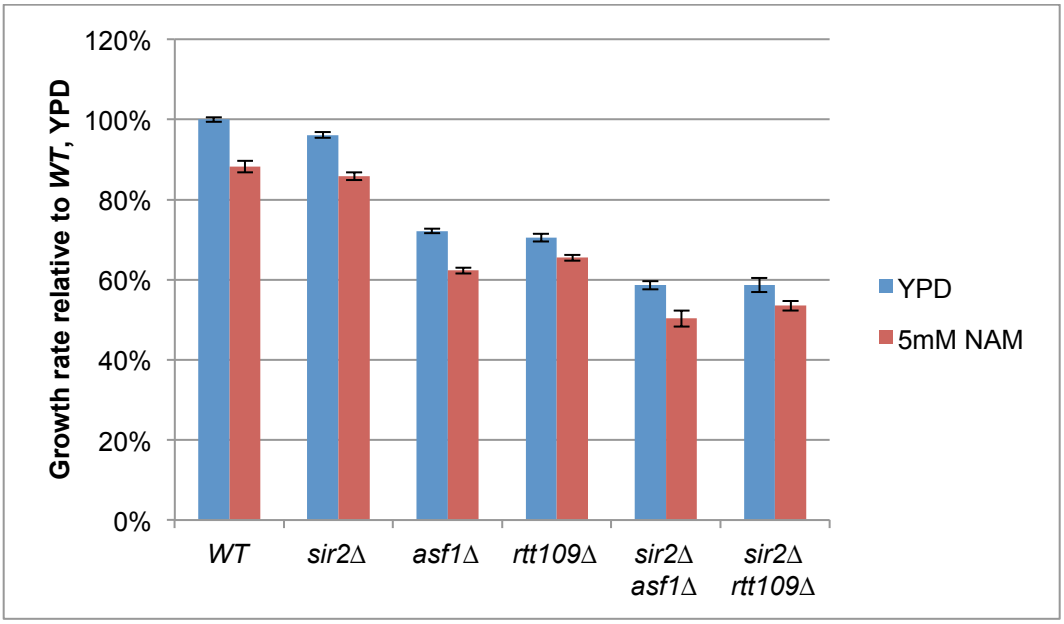


Figure AI.3: Growth rates of *sir2*Δ, *rtt109*Δ, and *asf1*Δ mutants in rich and 5mM nicotinamide media liquid culture
Logarithmically growing cells were seeded into 96-well plates in either YPD or 5mM nicotinamide media at 30°C and OD600 was assayed every 30 minutes to monitor growth. Growth rate was calculated based on OD600 values as described in (Mayfield et al., 2012). Growth rate is presented relative to wild-type. Data are from at least n=3 independent spores. Error bars depict standard error. All strains assayed are isogenic and progeny of a single diploid parent.

Discussion:

Genetic interactions identified by SGA require verification

High-throughput SGA analyses are prone to identifying false-positive interactions. The quantitative visual assay and tetrad-analysis method we employed is unlikely to recover false positives because we evaluated all products of meiosis and not only double-mutant progeny, as in SGA. We also worked with a small number of strains at any time to ensure that all the interactions we detected were repeatable, consistent, and statistically significant over a large sample size.

Our inability to recover the majority of *sir2*Δ genetic interactions identified by the Nyström lab SGA (Liu et al., 2010) could result from multiple factors. We performed our analysis in YPD media, not CSM media, as used by the Nyström lab. It is possible that nutritional conditions may be important to recover some *sir2*Δ genetic interactions and thus our tetrad analysis performed on YPD could be expected to have shown a different set of interactions than a SGA performed on CSM media. However, we tested 2 mutations described as interacting with *sir2*Δ on CSM and did not find significant SSL interactions so this cannot be a systematic explanation of the differences between our analysis and that of the Nyström lab. Importantly, we were able to recapitulate our findings related to *SIR2*, *ASF1*, and *RTT109* on CSM media and verified that regardless of media,

SIR2 and *ASF1* as well as *SIR2* and *RTT109* display SSL interactions with one another.

Lastly, it is possible that mutations in the specific yeast-deletion library, generated by growth or storage conditions either in our lab, or the Nyström lab, resulted in the suppression or creation of genetic-interaction phenotypes. Single-gene deletions in yeast bias individual strains to develop compensatory mutations elsewhere in the genome and this effect is exacerbated over time (Teng et al., 2013). The propensity for deletion mutants to acquire additional compensatory mutations over time may mean that the growth and storage conditions of the individual yeast-deletion collections used in any specific SGA substantively affect the outcome. Verification using tetrad analysis continues to be important for genetic interactions identified by SGA.

Interactions between Sir2 and a histone acetylation and incorporation pathway

Sir2 is important in the context of the Sir 2/3/4-silencing-complex for silencing of *HML*, *HMR*, and telomeres and in the RENT-complex to prevent recombination within rDNA. However, our data verified a Sir2-specific phenotype, dependent on Sir2 catalysis, independent of the Sir 2/3/4-complex. Cells lacking the function of either Rtt109 or Asf1 had lower fitness when Sir2 catalytic activity was also eliminated. The genetic interaction between *sir2*Δ and *asf1*Δ/*rtt109*Δ suggested that there could be a protein or histone substrate deacetylated by Sir2, whose increased level of acetylation, exacerbated the phenotype of *asf1*Δ or *rtt109*Δ mutants. It will be essential to determine if the fitness defect of *sir2*Δ *asf1*Δ and *sir2*Δ *rtt109*Δ double mutants proceeds through a histone substrate. It will be possible to test this hypothesis by determining if *sir2*Δ *asf1*Δ and *sir2*Δ *rtt109*Δ strains are phenocopied by constitutive histone aceylation and deactylation mimics such as *sir2*Δ H3K56Q and *sir2*Δ H3K56R.

The SLL interaction between *sir2*Δ and *rtt109*Δ/*asf1*Δ could operate through another mechanism as well. The visual appearance of the colonies and their sensitivity to hydroxy-urea and benomyl (data not shown) suggested the phenotype may be related to chromosome loss or segregation defects. A recent study shows that *rtt109*Δ strains display hyper-amplification of rDNA copy number (Ide et al., 2013). It is possible that the loss of Sir2 function, either alone or as a part of the RENT-complex, at the rDNA would exacerbate this condition, increasing rDNA recombination through a separate pathway, leading to a fitness defect. It will be important to test this hypothesis by creating *sir2*Δ *rtt109*Δ *fob1*Δ triple mutants to see if *fob1*Δ can rescue the *sir2*Δ dependent component of this phenotype back to levels of the *rtt109*Δ mutant alone.

Our study has demonstrated a robust, novel, silencing-independent function for Sir2 in combination with Asf1 and Rtt109. Future work will fully determine the specific cause and consequences of this interaction.

Materials and Methods:

Tetrad strain creation and selection

All strains used in this study are listed in Table AI.4 and were derived from S288c. All oligonucleotides used are listed in Table AI.5. Standard mating and sporulation techniques were used to perform yeast crosses, to generate diploids, and isolate tetrads. All yeast-deletion collection strains were verified using a geneA primer and kanB primer by PCR before mating to the *sir2*Δ query strain. Tetrads were dissected onto YPD medium and grown for 3-4 days before being photographed. After photography was completed, plates containing the dissected spores were replica plated onto selective media and individual spores were assigned genotypes based on the results.

ImageJ analysis

Images of tetrad plates were cropped, split into individual channels to isolate the red channel, and inverted. This procedure resulted in a white background with the individual spore colonies shown in black. This image was then analyzed using the ImageJ Analyze Particles function (Abramoff et el., 2004). The parameters were: size=3-infinity, show=particles. The resulting pixel-number values for each colony were then matched to colony genotype based on position. Student's t-tests were performed in Microsoft Excel. To label a SSL interaction between *sir2*Δ and a query gene (*yfg*Δ) as significant we required a significant ($p<.05$) difference via student's t-test between the pixel number of all colonies of all single-mutant *yfg*Δ and *sir2*Δ *yfg*Δ double mutants as well as between *sir2*Δ single mutants and *sir2*Δ *yfg*Δ double mutants. Query strains that did not satisfy both t-test requirements were not labeled as having a SSL interaction. All tetrad-assay data was based on the dissection and analysis of at least 40 complete tetrads from two independent diploids.

Plate reader growth assay

Logarithmically growing cells were seeded at OD600=.1 into YPD medium in 96-well plates and grown without shaking at 30° for 96 hours in a Versamax microplate reader. Analysis of plate reader growth data to determine growth rate was performed as described previously (Mayfield et al., 2012). Growth rate is presented relative to wild-type growth rate but all growth rates were initially calculated as Log_{10} doublings per hour. Nicotinamide was added at a concentration of 5mM in all NAM samples. Growth-rate data is based on at least n=3 independent spores from the same parent diploid. All strains assayed were generated from a single cross and are isogenic.

TableAI.4: Appendix yeast strains

Strain	Parent	Genotype	Source
JRY9532	S288c	*Y7092 (MATα can1Δ::STE2pr-Sp_his5 lyp1Δ ura3Δ0 leu2Δ0 his3Δ1 met15Δ0 LYS2+) sir2Δ::natMX4 hmra1-hmra2Δ::URA3 hmlα1-hmlα2Δ::hphMX4*	Liu et al., 2010
JRY9533	S288c	*MATα hmlΔ::HYGMX hmrΔ::URA3 his3Δ leu2Δ met15Δ ura3Δ*	This study
JRY9534	S288c	*MATα asf1Δ::KANMX hmlΔ::HYGMX hmrΔ::URA3 his3Δ leu2Δ met15Δ ura3Δ*	This study
JRY9535	S288c	*MATα rtt109Δ::KANMX hmlΔ::HYGMX hmrΔ::URA3 his3Δ leu2Δ met15Δ ura3Δ*	This study
JRY9536	S288c	*MATα asf1Δ::KANMX sir2Δ::NATMX hmlΔ::HYGMX hmrΔ::URA3 his3Δ leu2Δ met15Δ ura3Δ*	This study
JRY9537	S288c	*MATα rtt109Δ::KANMX sir2Δ::NATMX hmlΔ::HYGMX hmrΔ::URA3 his3Δ leu2Δ met15Δ ura3Δ*	This study
JRY9538	S288c	*MATα asf1Δ::KANMX rtt109Δ::KANMX hmlΔ::HYGMX hmrΔ::URA3 his3Δ leu2Δ met15Δ ura3Δ*	This study
JRY9539	S288c	*MATα asf1Δ::KANMX rtt109Δ::KANMX sir2Δ::NATMX hmlΔ::HYGMX hmrΔ::URA3 his3Δ leu2Δ met15Δ ura3Δ*	This study
JRY9540	S288c	*MATα sir2Δ::NATMX hmlΔ::HYGMX hmrΔ::URA3 his3Δ leu2Δ met15Δ ura3Δ*	This study
JRY9541	S288c	*MATα can1Δ::STE2pr-Sp_his5 lyp1Δ ura3Δ0 leu2Δ0 his3Δ1 met15Δ0 LYS2+ sir2Δ::natMX4 hmra1-hmra2Δ::URA3 hmlα1-hmlα2Δ::hphMX4 / MATa asf1Δ::KANMX his3Δ leu2Δ met15Δ ura3Δ*	This study
JRY9542	S288c	*MATα can1Δ::STE2pr-Sp_his5 lyp1Δ ura3Δ0 leu2Δ0 his3Δ1 met15Δ0 LYS2+ sir2Δ::natMX4 hmra1-hmra2Δ::URA3 hmlα1-hmlα2Δ::hphMX4 / MATa rtt109Δ::KANMX his3Δ leu2Δ met15Δ ura3Δ*	This study
JRY9543	S288c	*MATα can1Δ::STE2pr-Sp_his5 lyp1Δ ura3Δ0 leu2Δ0 his3Δ1 met15Δ0 LYS2+ sir2Δ::natMX4 hmra1-hmra2Δ::URA3 hmlα1-hmlα2Δ::hphMX4 / MATa cac2Δ::KANMX his3Δ leu2Δ met15Δ ura3Δ*	This study
JRY9544	S288c	*MATα can1Δ::STE2pr-Sp_his5 lyp1Δ ura3Δ0 leu2Δ0 his3Δ1 met15Δ0 LYS2+ sir2Δ::natMX4 hmra1-hmra2Δ::URA3 hmlα1-hmlα2Δ::hphMX4 / MATa swr1Δ::KANMX his3Δ leu2Δ met15Δ*	This study

		ura3Δ	
JRY9545	S288c	*MATα can1Δ::STE2pr-Sp_his5 lyp1Δ ura3Δ0 leu2Δ0 his3Δ1 met15Δ0 LYS2+ sir2Δ::natMX4 hmra1-hmra2Δ::URA3 hmlα1-hmlα2Δ::hphMX4 / MATa slx8Δ::KANMX his3Δ leu2Δ met15Δ ura3Δ*	This study
JRY9546	S288c	*MATα can1Δ::STE2pr-Sp_his5 lyp1Δ ura3Δ0 leu2Δ0 his3Δ1 met15Δ0 LYS2+ sir2Δ::natMX4 hmra1-hmra2Δ::URA3 hmlα1-hmlα2Δ::hphMX4 / MATa ctf4Δ::KANMX his3Δ leu2Δ met15Δ ura3Δ*	This study
JRY9547	S288c	*MATα can1Δ::STE2pr-Sp_his5 lyp1Δ ura3Δ0 leu2Δ0 his3Δ1 met15Δ0 LYS2+ sir2Δ::natMX4 hmra1-hmra2Δ::URA3 hmlα1-hmlα2Δ::hphMX4 / MATa elp4Δ::KANMX his3Δ leu2Δ met15Δ ura3Δ*	This study
JRY9548	S288c	*MATα can1Δ::STE2pr-Sp_his5 lyp1Δ ura3Δ0 leu2Δ0 his3Δ1 met15Δ0 LYS2+ sir2Δ::natMX4 hmra1-hmra2Δ::URA3 hmlα1-hmlα2Δ::hphMX4 / MATa hst1Δ::KANMX his3Δ leu2Δ met15Δ ura3Δ*	This study
JRY9549	S288c	*MATα can1Δ::STE2pr-Sp_his5 lyp1Δ ura3Δ0 leu2Δ0 his3Δ1 met15Δ0 LYS2+ sir2Δ::natMX4 hmra1-hmra2Δ::URA3 hmlα1-hmlα2Δ::hphMX4 / MATa hst3Δ::KANMX his3Δ leu2Δ met15Δ ura3Δ*	This study
JRY9550	S288c	*MATα can1Δ::STE2pr-Sp_his5 lyp1Δ ura3Δ0 leu2Δ0 his3Δ1 met15Δ0 LYS2+ sir2Δ::natMX4 hmra1-hmra2Δ::URA3 hmlα1-hmlα2Δ::hphMX4 / MATa mdm12Δ::KANMX his3Δ leu2Δ met15Δ ura3Δ*	This study
JRY9551	S288c	*MATα can1Δ::STE2pr-Sp_his5 lyp1Δ ura3Δ0 leu2Δ0 his3Δ1 met15Δ0 LYS2+ sir2Δ::natMX4 hmra1-hmra2Δ::URA3 hmlα1-hmlα2Δ::hphMX4 / MATa mek1Δ::KANMX his3Δ leu2Δ met15Δ ura3Δ*	This study
JRY9552	S288c	*MATα can1Δ::STE2pr-Sp_his5 lyp1Δ ura3Δ0 leu2Δ0 his3Δ1 met15Δ0 LYS2+ sir2Δ::natMX4 hmra1-hmra2Δ::URA3 hmlα1-hmlα2Δ::hphMX4 / MATa nup2Δ::KANMX his3Δ leu2Δ met15Δ ura3Δ*	This study
JRY9553	S288c	*MATα can1Δ::STE2pr-Sp_his5 lyp1Δ ura3Δ0 leu2Δ0 his3Δ1 met15Δ0 LYS2+ sir2Δ::natMX4 hmra1-hmra2Δ::URA3 hmlα1-hmlα2Δ::hphMX4 / MATa pho88Δ::KANMX his3Δ leu2Δ met15Δ ura3Δ*	This study

JRY9554	S288c	*MATα can1Δ::STE2pr-Sp_his5 lyp1Δ ura3Δ0 leu2Δ0 his3Δ1 met15Δ0 LYS2+ sir2Δ::natMX4 hmra1-hmra2Δ::URA3 hmlα1-hmlα2Δ::hphMX4 / MATa slx9Δ::KANMX his3Δ leu2Δ met15Δ ura3Δ*	This study
JRY9555	S288c	*MATα can1Δ::STE2pr-Sp_his5 lyp1Δ ura3Δ0 leu2Δ0 his3Δ1 met15Δ0 LYS2+ sir2Δ::natMX4 hmra1-hmra2Δ::URA3 hmlα1-hmlα2Δ::hphMX4 / MATa swc5Δ::KANMX his3Δ leu2Δ met15Δ ura3Δ*	This study
JRY9556	S288c	*MATα can1Δ::STE2pr-Sp_his5 lyp1Δ ura3Δ0 leu2Δ0 his3Δ1 met15Δ0 LYS2+ sir2Δ::natMX4 hmra1-hmra2Δ::URA3 hmlα1-hmlα2Δ::hphMX4 / MATa yjl055wΔ::KANMX his3Δ leu2Δ met15Δ ura3Δ*	This study
JRY9557	S288c	*MATα can1Δ::STE2pr-Sp_his5 lyp1Δ ura3Δ0 leu2Δ0 his3Δ1 met15Δ0 LYS2+ sir2Δ::natMX4 hmra1-hmra2Δ::URA3 hmlα1-hmlα2Δ::hphMX4 / MATa ama1Δ::KANMX his3Δ leu2Δ met15Δ ura3Δ*	This study
JRY9558	S288c	*MATα lyp1Δ ura3Δ0 leu2Δ0 his3Δ1 met15Δ0 LYS2+ sir4Δ::natMX4 hmra1-hmra2Δ::URA3 hmlα1-hmlα2Δ::hphMX4*	This study
JRY9559	S288c	*MATα lyp1Δ ura3Δ0 leu2Δ0 his3Δ1 met15Δ0 LYS2+ sir3Δ::natMX4 hmra1-hmra2Δ::URA3 hmlα1-hmlα2Δ::hphMX4*	This study
JRY9560	S288c	*MATα lyp1Δ ura3Δ0 leu2Δ0 his3Δ1 met15Δ0 LYS2+ sir4Δ::natMX4 hmra1-hmra2Δ::URA3 hmlα1-hmlα2Δ::hphMX4 / MATa asf1Δ::KANMX his3Δ leu2Δ met15Δ ura3Δ*	This study
JRY9561	S288c	*MATα lyp1Δ ura3Δ0 leu2Δ0 his3Δ1 met15Δ0 LYS2+ sir3Δ::natMX4 hmra1-hmra2Δ::URA3 hmlα1-hmlα2Δ::hphMX4 / MATa asf1Δ::KANMX his3Δ leu2Δ met15Δ ura3Δ*	This study
JRY9562	S288c	*MATα lyp1Δ ura3Δ0 leu2Δ0 his3Δ1 met15Δ0 LYS2+ sir4Δ::natMX4 hmra1-hmra2Δ::URA3 hmlα1-hmlα2Δ::hphMX4 / MATa rtt109Δ::KANMX his3Δ leu2Δ met15Δ ura3Δ*	This study
JRY9563	S288c	*MATα lyp1Δ ura3Δ0 leu2Δ0 his3Δ1 met15Δ0 LYS2+ sir3Δ::natMX4 hmra1-hmra2Δ::URA3 hmlα1-hmlα2Δ::hphMX4 / MATa rtt109Δ::KANMX his3Δ leu2Δ met15Δ ura3Δ*	This study
JRY9564	S288c	*MATα lyp1Δ ura3Δ0 leu2Δ0 his3Δ1 met15Δ0 LYS2+ sir2Δ::natMX4 hmra1-hmra2Δ::URA3 hmlα1-hmlα2Δ::hphMX4 leu2 :: sir2N345A*	This study
JRY9565	S288c	*MATα lyp1Δ ura3Δ0 leu2Δ0 his3Δ1 met15Δ0*	This

		LYS2+ sir2Δ::natMX4 hmra1-hmra2Δ::URA3 hmlα1-hmlα2Δ::hphMX4 leu2 :: sir2N345A / MATa asf1Δ::KANMX his3Δ leu2Δ met15Δ ura3Δ	study
JRY9566	S288c	*MATα lyp1Δ ura3Δ0 leu2Δ0 his3Δ1 met15Δ0 LYS2+ sir2Δ::natMX4 hmra1-hmra2Δ::URA3 hmlα1-hmlα2Δ::hphMX4 leu2 :: sir2N345A / MATa rtt109Δ::KANMX his3Δ leu2Δ met15Δ ura3Δ*	This study

TableAI.5: Appendix oligonucleotides

Name	**Sequence**
kan B	CTGCAGCGAGGAGCCGTAAT
ASF1 A	AATGCTGTTTTATTCCGTTCTTACA
RTT109 A	TCTCCTAAAATCGATCAAGATATGG
CAC2 A	GAAGGAATAGATTTCTGTGGTGAAA
SWR1 A	CCTCTATACGATTATTAAGGGAGGG
SLX8 A	AAGAGAACAGTAAGCATGAGAGGAA
CTF4 A	GTGAAATCGTAGTTTGCCTGATACT
ELP4 A	GCGATAATCAAGGAGAATATCAGTG
HST1 A	ATCTACAAAATCAAGTGGACACACA
HST3 A	AAAGTTCATCACCTTCCTTAGCAC
MDM12 A	CTTATATTGGGCAACTTCTGACACT
MEK1 A	CAATATTGACTGATAGCGATCTCCT
NUP2 A	CAACAATAAAATCCCAGCAATTATC
PHO88 A	AGAAGAAGAACATCACTTTACACGG
SLX9 A	TAGAGCTGCTATGGCTGTTGTAATA
SWC5 A	TTACAGAAAGATTATTTAATGCCGC
YJL055W A	CTTCTTTACCTATCGTCAGAGCATC
AMA1 A	AATGCCTCTATGTCACCTTCAATAG

Appendix references

Abramoff, M.D., Magalhaes, P.J., Ram, S.J. "Image Processing with ImageJ". Biophotonics International, volume 11, issue 7, pp. 36-42, 2004.

Armstrong, C.M., Kaeberlein, M., Imai, S.I., and Guarente, L. (2002). Mutations in *Saccharomyces cerevisiae* gene *SIR2* can have differential effects on *in vivo* silencing phenotypes and *in vitro* histone deacetylation activity. Mol. Biol. Cell *13*, 1427–1438.

Collins, S.R., Miller, K.M., Maas, N.L., Roguev, A., Fillingham, J., Chu, C.S., Schuldiner, M., Gebbia, M., Recht, J., Shales, M., et al. (2007). Functional dissection of protein complexes involved in yeast chromosome biology using a genetic interaction map. Nature *446*, 806–810.

Collins, S.R., Schuldiner, M., Krogan, N.J., and Weissman, J.S. (2006). A strategy for extracting and analyzing large-scale quantitative epistatic interaction data. Genome Biology *7*, R63.

Costanzo, M., Baryshnikova, A., Bellay, J., Kim, Y., Spear, E.D., Sevier, C.S., Ding, H., Koh, J.L.Y., Toufighi, K., Mostafavi, S., et al. (2010). The Genetic Landscape of a Cell. Science *327*, 425–431.

Driscoll, R., Hudson, A., and Jackson, S.P. (2007). Yeast Rtt109 Promotes Genome Stability by Acetylating Histone H3 on Lysine 56. Science *315*, 649–652.

Han, J., Zhou, H., Li, Z., Xu, R.M., and Zhang, Z. (2007). The Rtt109-Vps75 Histone Acetyltransferase Complex Acetylates Non-nucleosomal Histone H3. Journal of Biological Chemistry *282*, 14158–14164.

Ide, S., Saka, K., and Kobayashi, T. (2013). Rtt109 Prevents Hyper-Amplification of Ribosomal RNA Genes through Histone Modification in Budding Yeast. PLoS Genet *9*, e1003410.

Koh, J.L.Y., Ding, H., Costanzo, M., Baryshnikova, A., Toufighi, K., Bader, G.D., Myers, C.L., Andrews, B.J., and Boone, C. (2009). DRYGIN: a database of quantitative genetic interaction networks in yeast. Nucleic Acids Research *38*, D502–D507.

Kolonko, E.M., Albaugh, B.N., Lindner, S.E., Chen, Y., Satyshur, K.A., Arnold, K.M., Kaufman, P.D., Keck, J.L., and Denu, J.M. (2010). Catalytic activation of histone acetyltransferase Rtt109 by a histone chaperone. Proceedings of the National Academy of Sciences *107*, 20275–20280.

Liu, B., Larsson, L., Caballero, A., Hao, X., Öling, D., Grantham, J., and Nyström, T. (2010). The Polarisome Is Required for Segregation and Retrograde Transport of Protein Aggregates. Cell *140*, 257–267.

Mayfield, J.A., Davies, M.W., Dimster-Denk, D., Pleskac, N., McCarthy, S., Boydston, E.A., Fink, L., Lin, X.X., Narain, A.S., Meighan, M., et al. (2012). Surrogate Genetics and Metabolic Profiling for Characterization of Human Disease Alleles. Genetics *190*, 1309–1323.

Rine, J., and Herskowitz, I. (1987). Four genes responsible for a position effect on expression from *HML* and *HMR* in *Saccharomyces cerevisiae*. Genetics *116*, 9–22.

Schuldiner, M., Collins, S.R., Thompson, N.J., Denic, V., Bhamidipati, A., Punna, T., Ihmels, J., Andrews, B., Boone, C., Greenblatt, J.F., et al. (2005). Exploration of the Function and Organization of the Yeast Early Secretory Pathway through an Epistatic Miniarray Profile. Cell *123*, 507–519.

Sharp, J.A., Fouts, E.T., Krawitz, D.C., and Kaufman, P.D. (2001). Yeast histone deposition protein Asf1p requires Hir proteins and PCNA for heterochromatic silencing. Curr. Biol. *11*, 463–473.

Teng, X., Dayhoff-Brannigan, M., Cheng, W.-C., Gilbert, C.E., Sing, C.N., Diny, N.L., Wheelan, S.J., Dunham, M.J., Boeke, J.D., Pineda, F.J., et al. (2013). Genome-wide Consequences of Deleting Any Single Gene. Molecular Cell *52*, 485–494.

Tong, A.H., Evangelista, M., Parsons, A.B., Xu, H., Bader, G.D., Pagé, N., Robinson, M., Raghibizadeh, S., Hogue, C.W., Bussey, H., et al. (2001). Systematic genetic analysis with ordered arrays of yeast deletion mutants. Science *294*, 2364–2368.

Tong, A.H.Y., Lesage, G., Bader, G.D., Ding, H., Xu, H., Xin, X., Young, J., Berriz, G.F., Brost, R.L., Chang, M., et al. (2004). Global mapping of the yeast genetic interaction network. Science *303*, 808–813.

Tsubota, T., Berndsen, C.E., Erkmann, J.A., Smith, C.L., Yang, L., Freitas, M.A., Denu, J.M., and Kaufman, P.D. (2007). Histone H3-K56 Acetylation Is Catalyzed by Histone Chaperone-Dependent Complexes. Molecular Cell *25*, 703–712.

Winzeler, E.A., Shoemaker, D.D., Astromoff, A., Liang, H., Anderson, K., Andre, B., Bangham, R., Benito, R., Boeke, J.D., Bussey, H., et al. (1999). Functional characterization of the *S. cerevisiae* genome by gene deletion and parallel analysis. Science *285*, 901–906.